

LINEAR DICHROISM AND ORIENTATION
OF THE PHYCOMYCES PHOTOPIGMENT

- I. Response and Absorption Studies
- II. Fluorescence Studies

Thesis by
Algirdas J. Jesaitis

In Partial Fulfillment of the Requirements
for the Degree
Doctor of Philosophy

California Institute of Technology
Pasadena, California
1973

(Submitted April 18, 1973)

Mano

Motinai, Tėvui,

Broliai,

Dėdėms, ypač Dėdei Margeriui,

ir

Tetoms

su meile skiriu

ACKNOWLEDGEMENTS

My warmest thanks go to Max Delbrück for his guidance and encouragement throughout my years at Caltech and for his invaluable suggestions and hard work on this thesis. Though a part of this guidance took the form of kicks to the seat of my pants, I am certain I benefited from the whole experience by exposure to the patience, insight, and perspicuity that I have admired for so long.

I feel special indebtedness to Prof. Edward S. Castle, though I have never even met him. Forty-one years ago he discovered the polarized light effect in *Phycomyces* and started a running controversy that has now produced this thesis.

I would also like to thank:

Dr. Michael W. Berns for the equipment, help and encouragement he provided in the laser excited fluorescence studies,
Prof. Sten Samson for the use of his microscope,
the late Prof. J. H. Sturdivant for laboratory space and helpful discussions on polarizing optics,
Mae Ramirez for her conscientious and accurate typing,
and the U. S. Government for supporting my stay at Caltech.

Many more thanks go to my friends and colleagues down in the *Phycomyces* caverns for their day to day help, conversation, and good humor. My special thanks go to:

Bill Goodell for bringing some Colorado down there,
Ken Foster, Bob Cohen, and Ed Lipson for their biophysics,

Ruth Dusenbery for her sympathy and help on this thesis,
Tomatsu Ootaki for the excitement and laughter he cultivated,
and of course, Jeanette Navest and Bertha Jones for their cheer-
fulness, hard work and monthly 2 p.m. celebrations.

Most of all I want to thank my friends at Tech--especially Jack for the
five plus long years of jokes, commiseration and solid friendship, Les
for her companionship and understanding, and of course, the Prufrocks--
without them I doubt very much if this thesis would have ever been
written.

ABSTRACT

The response of five strains of the fungus Phycomyces to linearly polarized light was studied. The sporangiophores of the strains, C2, C5, C9, C158, and NRRL 1555 (wildtype) differed primarily in optical attenuation. Their abilities to distinguish between longitudinally and transversely polarized blue light were found to be approximately the same.

The angle (with respect to the transverse axis) at which the \vec{E} vector of the polarized light must be oriented to give a maximum response during perpendicular incidence into the cell was measured. It was found to be $42^\circ \pm 3^\circ$ for 280 nm light in the wild type strain. In the C158 strain this angle was $7^\circ \pm 3^\circ$ at 456 nm and $7 \pm 8^\circ$ at 486 nm.

The in vivo attenuation of polarized light as a function of the angle between the \vec{E} vector and the cell axis was measured. The maximum transmission differences resulting from anisotropic attenuation were $4 \pm 2\%$ at 320 nm, $3 \pm 2\%$ at 456 nm, and $2 \pm 1\%$ at 486 nm.

These results indicate that the polarized light effect in Phycomyces cannot arise from reflections at the cell surface, nor from attenuations due to internal screening or scattering and, therefore, must be due to the dichroism and orientation of the visual pigment.

An attempt was made to detect the presence of the photopigment in cell wall and plasmalemma fractions using fluorescence kinetics and polarization. Excitation of these preparations with high intensity 488 nm laser light and monitoring fluorescence intensity with a microphotometer, a fluorescence decay and a periodic dependence of fluores-

cence intensity on the \vec{E} vector angle of exciting light was found. The relevance of this fluorescence to the in vivo photosystem is questionable because of the high excitation intensity necessary to produce any detectable fluorescence.

TABLE OF CONTENTS

PART	TITLE	PAGE
	Acknowledgments.....	ii
	Abstract.....	v
	List of Illustrations.....	x
	List of Tables.....	xii
I.	RESPONSE AND ABSORPTION STUDIES.....	1
	<u>Introduction</u>	2
	general.....	2
	linear dichroism.....	5
	interaction of polarized light and biological systems.....	7
	interaction of polarized light and <u>Phycomyces</u>	9
	<u>Materials and Methods</u>	13
	Strains.....	13
	Growth Media.....	13
	Culture Conditions.....	13
	Light Sources.....	13
	Polarization.....	16
	Intensity.....	17
	Physiological Experiments.....	17
	Microspectrophotometry.....	23
	<u>Results</u>	28
	A. Differential growth responses of wild	

type and mutants to longitudinally and transversely polarized broad band blue light.....	28
B. Microspectrophotometry.....	34
C. \vec{E} -vector angle of maximum response at 280 nm, 456 nm, and 486 nm.....	34
<u>Discussion</u>	45
The Fresnel Effect.....	45
Anisotropic Attenuation.....	48
Oriented Dichroic Receptors.....	48
Perfectly Aligned Dipoles.....	49
Flavin Receptor, 280 nm and 455 nm dipoles separated by 60°	60
Partially Disordered Receptor Molecules.	63
Conclusions.....	71
<u>Appendix I</u> - Calculation of \bar{r} , σ for the dif- ferential growth response.....	73
<u>Appendix II</u> - Dipole orientation and dichroic effects.....	77
A. Relative differential absorption.....	81
B. The angle of maximum D, (θ_{\max}).....	81
C. The angle, γ , between absorption dipoles, \vec{e}_1 and \vec{e}_2	82
D. Mixture of aligned and randomly oriented dipoles.....	83

II.	FLUORESCENCE STUDIES.....	86
	<u>Purpose</u>	87
	<u>Introduction</u>	88
	<u>Materials and Methods</u>	90
	Apparatus.....	90
	Specimens and preparation.....	90
	Fluorescence measurements.....	93
	<u>Results</u>	94
	<u>Discussion and Conclusion</u>	98
	BIBLIOGRAPHY.....	100

LIST OF ILLUSTRATIONS

FIGURE	TITLE	PAGE
1	Phototropic and growth response action spectrum of <u>Phycomyces</u>	3
2	Illumination arrangement and growth response.	19
3	Growth responses to polarized light and in- tensity alternations.....	21
4	Apparatus for light programs.....	24
5	Growth response versus intensity differen- tials.....	32
6	Sporangiophore absorption spectra.....	37
7	Polarized light responses versus θ , at high optical density.....	41
8	Oblique and normal views of hypothetical receptor transition dipole orientation..	50
9	Possible receptor dipole orientation.....	53
10	Theoretical receptor dichroism.....	56
11	Relative magnitudes of the radial and tangen- tial components of the receptor dipole..	58
12	Assumed directions of transition moments in riboflavin.....	61
13	Orientation of tangential components of pairs of receptor dipoles constrained to lie 60° apart.....	64
14	Fractional random orientation constraint, U,	

	plotted as a function of ϕ_{456}	67
15	Relative amplitude of growth rate variation (r).....	74
16	Coordinate definitions.....	78
17	Microfluorimeter.....	91
18	Fluorescence decay and polarization results..	95

LIST OF TABLES

NUMBER	TITLE	PAGE
I	Strains of <u>Phycomyces blakesleeanus</u> used in this work.....	14
II	Growth Media.....	15
III	Average responses of 5 strains to alternating 5 minute periods of longitudinally and transversely polarized blue light.....	30
IV	<u>In vivo</u> absorbance values at 500 nm and 450 nm for 5 strains.....	35
V	Polarized light absorption anisotropy.....	36
VI	\vec{E} vector angles for maximum response.....	43

PART I

RESPONSE AND ABSORPTION STUDIES

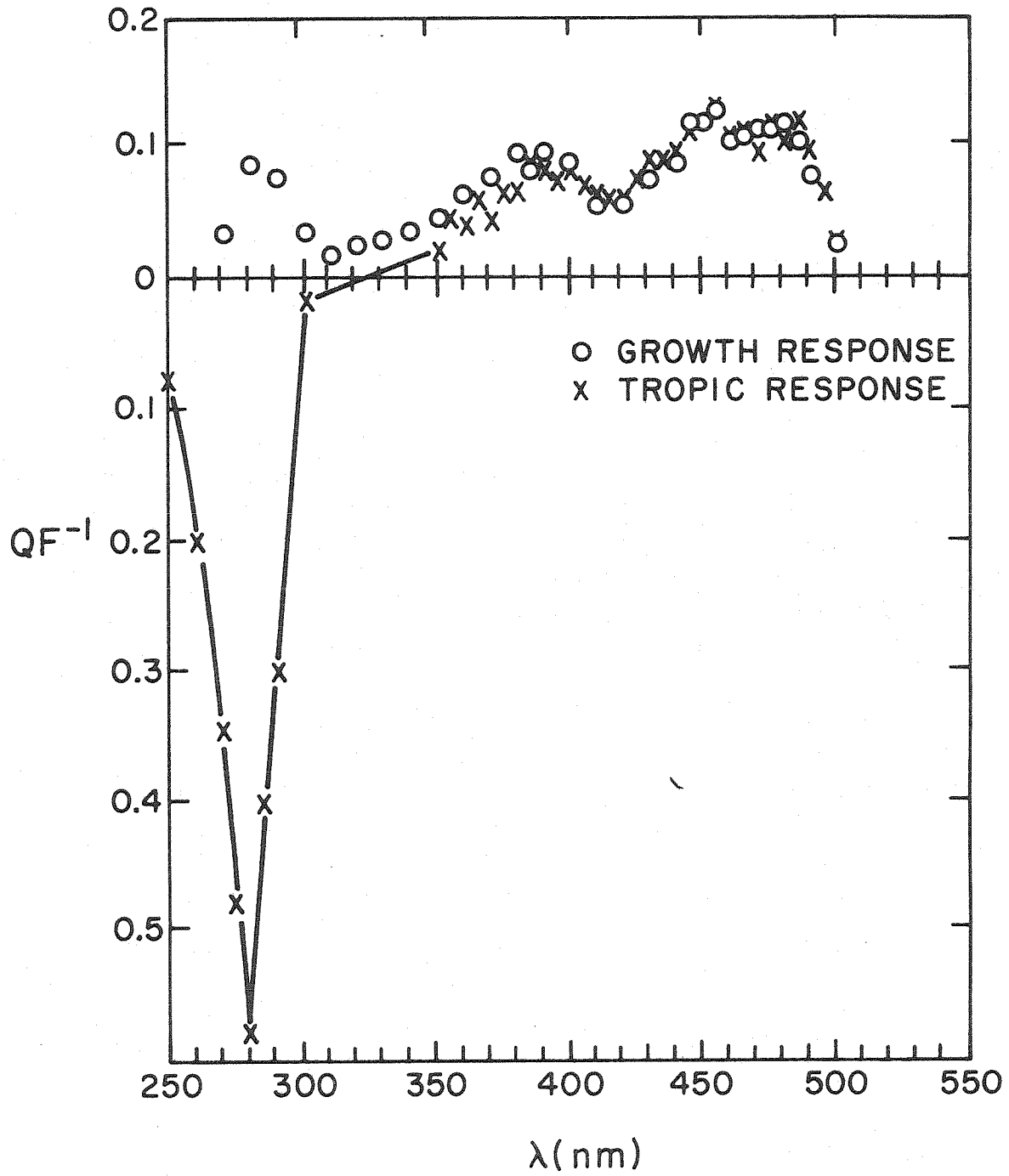
INTRODUCTION

There exist a wide variety of processes in organisms which are blue light sensitive. Among these are photoperiodism in insects (Zimmerman and Ives, 1971; Lees, 1968); carotenoid synthesis in nonphotosynthetic plants (Batra, 1971); spore germination in fungi and ferns (Jaffe and Etzold, 1962); zygote germination in algae (Jaffe, 1958); photosynthetic and metabolic regulation in green plants (Voskrenskaya, 1972); phototaxis in microorganisms (Clayton, 1965); and phototropism in plants (Thomas, 1965). Nearly all those investigated have a wavelength dependence or action spectrum which is very similar (Bergman et al., 1969, p. 135). It is believed that they are mediated by a common primary photoreceptor mechanism.

Phycomyces exhibits this type of blue sensitivity in its phototropic and growth responses as well as in its development. The former two responses have been well characterized by a detailed action spectrum (Fig. 1) and extensive response studies (Bergman et al., 1969, pp. 119-141). All seem to indicate that either a flavin or carotenoid is responsible for the primary absorption of light and activation of the mechanisms leading to the respective outputs. An insight into the molecular basis of blue light effects in this organism may have a universal bearing on all of the blue light sensitive systems.

Any discussion of a photoreceptor must include mention of its location and orientation in vivo, if an understanding of its function is to be reached. This is especially true since in many light sensitive systems the receptors are closely associated with a membrane. The inter-

Figure 1. Phycomyces action spectra for the phototropic and growth responses determined by the null method (i.e., quantum flux at which the standard and test stimuli are indistinguishable). Taken from Delbrück and Shropshire (1960).



action between polarized light and the photosensitive systems has been used to determine the orientation and location of the receptors. This has been possible because virtually all biologically important photosensitive molecules are linearly dichroic (Jaffe and Etzold, 1965).

Linear dichroism is the preferential absorption of linearly polarized light in a particular direction. A linearly dichroic medium is characterized by three principal axes of absorption. Light will be absorbed maximally along one of these. The two other mutually perpendicular axes will, in general, absorb to a lesser extent. This implies that absorption can be represented as a triaxial ellipsoid. The radius of the ellipsoid represents a measure of the absorption at some orientation of the electric vector of the light with respect to the medium. Since the medium is usually fixed for measurement, only the projection of the ellipsoid on to the plane perpendicular to the measuring beam is detected. This will usually be characterized by two absorbancies d_{\parallel} and d_{\perp} . \parallel means that \vec{E} , the electric vector of the polarized light, is parallel to the major axis; \perp means that it is perpendicular to this axis. The quotient $\frac{d_{\parallel} - d_{\perp}}{d_{\parallel} + d_{\perp}}$ is called the dichroism of the system and d_{\parallel}/d_{\perp} , the dichroic ratio.

The linear dichroism of a medium is a result of the ordering of the asymmetrically absorbing molecules. These molecules are characterized by linear absorbing groups (e.g., linear systems of conjugated double bonds). Some examples of such molecules are aromatic hydrocarbons, anthracene-like dyes, carotenoids, and tetrapyrroles. Quantum mechanically, such systems exhibit large absorption transition moments. This quantity represents the charge migration during a transition from

the ground to the excited state of the molecule. Light polarized at an angle θ to the direction of the moment, will have a probability of exciting a transition proportion to $\cos^2 \theta$. Thus, a fully aligned molecule will have an infinite dichroic ratio (dichroism = 1). In reality, it will be finite (dichroism < 1) because of molecular rotation, vibration, and angular distribution relative to the incident light.

$\pi \rightarrow \pi^*$ and $n \rightarrow \pi^*$ are biologically important transitions exhibiting nonzero transition moments in the visible and ultraviolet. The $\pi \rightarrow \pi^*$ transition arises from promotion of a delocalized π orbital electron of a conjugated system to the higher energy, antibonding π^* orbital. Since the wave functions of the π and π^* states, ϕ_π and ϕ_{π^*} , are both antisymmetric with respect to reflection in the plane determined by the conjugated system, the electric dipole moment operator, \vec{M} , must be symmetric in order that the transition probability integral $\int \phi_\pi \vec{M} \phi_{\pi^*} d\tau$ be nonzero. Thus if \vec{M} lies in the plane of the bonds, it will be symmetric and the transition will have a nonzero probability. An n, or nonbonding orbital from a heteroatom (N, O) in the conjugated system, is usually in the plane of the bonds and, therefore, is symmetric. Thus \vec{M} has to be antisymmetric, that is, perpendicular to the plane of the bonds for $\int \phi_n \vec{M} \phi_{\pi^*} d\tau$ to be nonzero. Consequently, E must be parallel to the plane in order to excite a $\pi \rightarrow \pi^*$ transition and normal to the plane in order to excite a $n \rightarrow \pi^*$ transition (Seliger and McElroy, 1965).

Nearly all of the molecules responsible for photosensitivity in organisms contain these conjugated systems: DNA, chlorophyll, rhodopsin, porphyrin, phytochrome, carotenoids, and flavins are some examples. Solutions of any of these, however, will show no anisotropy in absorption.

For any given orientation of \vec{E} there will be an equal number of molecules with absorption axes aligned in this direction. Consequently, absorption will be independent of polarization.

Organisms are highly structured and show organization of their components into various organelles. These show a great deal of ordering on both the morphological and the molecular levels. Photosensitive molecules in most cases are associated with these structures and are likewise ordered; they should, therefore, exhibit dichroism macroscopically.

There have been many demonstrations of dichroism and ordering of photosensitive pigments in both plant and animal cells. Liebman (1962) has shown using in situ microspectrophotometric studies of single retinal rods of frogs, that rhodopsin is oriented and dichroic. Blasie and Worthington (1969) localized the photopigment to the disk membrane of the rods and described its planar arrangement. In a recent paper, Blasie (1972) describes the further localization of this pigment relative to the lipid hydrocarbon core of the membrane.

In invertebrates, the dichroism and orientation of the visual pigment in crayfish rhabdoms has been demonstrated by microspectrophotometric measurements (Waterman et al., 1969) and by studies of the organism's response to polarized light (Waterman, 1966). Here it was also postulated that the pigment was associated with the membrane in a planar or tangential order.

In green plants, a great deal of information has been collected about the location and orientation of chlorophyll. Olson (1963) demonstrated molecular orientation of chlorophyll in vivo by utilizing

the spectral dependence of dichroism and fluorescence polarization of chloroplasts. The chlorophyll has been shown to be intimately associated with the chloroplast lamellae (Menke, 1963), giving rise to a highly ordered molecular array exhibiting efficient energy transfer from one chlorophyll to another (Robinson, 1966).

Phytochrome, the molecule responsible for red light photoregulation in plants, has been shown to be oriented with respect to the cell axis and localized in the plasma membrane of the filamentous green alga, Mougeotia (Haupt, et al. 1969). Linearly polarized red and far red microbeams stimulated localized chloroplast movement. Plasma membrane irradiated by longitudinally polarized red light attracted chloroplasts. Membrane exposed to transversely polarized far red light repelled them. The orthogonal polarizations had no effect. This revealed the dichroism, orientation and location of the phytochrome.

Jaffe and Etzold (1965) reported a response to polarized red light in the germination of spores of the moss Funaria. By a series of experiments using various orientations, intensities, and spectral distributions of polarized light, they showed that some of the phytochrome responsible for the effect was tangentially ordered. Nebel (1969) demonstrated that the phototropic protenema of the moss Physcomitrium, likewise, had tangentially oriented phytochrome in both the red and far red absorbing forms.

Blue light regulated organisms are believed to have either a flavin or carotenoid as the photoreceptor. Since these have conjugated bond systems, they too should exhibit sensitivity to polarized light. Indeed, spores of the fungus Botrytis and the fern Osmunda exhibit

strong germination responses to polarized blue light (Jaffe and Etzold, 1962). From this it was deduced that these spores have ordered photoreceptors located near the cell surface. Jaffe (1958) also demonstrated a similar type of response in the zygote of the brown alga Fucus and concluded tangential photoreceptor ordering.

Zurzycki (1967a) reported that Funaria chloroplasts exhibited a response to polarized blue light. He found that the chloroplasts migrated to cell walls parallel to \vec{E} . Absorption spectroscopy in cell fractions provided some evidence that the receptors were localized near the cell wall (Zurzycki, 1967b).

In summary then, it may be stated that virtually all biological photosensitive processes are governed by dichroic molecules. These molecules are usually associated with a membrane in the cell and, as a consequence, exhibit a varying degree of orientation and dichroism, depending on the organism in which they reside.

A Phycomyces sporangiophore (spph) responds less to longitudinally polarized light (\vec{E} is parallel to the long axis of the spph cylinder) than to transversely polarized light. When illuminated from opposite sides by longitudinally and transversely polarized light, the longitudinal beam must be 10% more intense than the transverse beam to prevent phototropic bending (Castle, 1934). In a different experiment measuring the light growth response, the longitudinal beam, at a wavelength of 450 nm, must be $24 \pm 4\%$ more intense than the transverse beam in order to produce uniform growth. At 380 nm this figure is $21 \pm 6\%$ (Shropshire, 1959).

Castle concluded that this effect is due to differential reflection losses (see Discussion) and not to dichroism of oriented receptors. Shropshire added strength to this conclusion by showing that the greater effectiveness of the transverse beam in producing a growth response is reduced to $6 \pm 6\%$ when the sph is placed in a medium of approximately matching refractive index. In such a medium, reflection is nearly eliminated. He also thought that it would be unlikely that a dichroic receptor molecule be equally dichroic at two different wavelengths.

Jaffe (1960) contested the validity of these arguments. Using a theoretical analysis, he showed how Castle's phototropic result and Shropshire's growth response results could be explained by the dichroic oriented receptor hypothesis, and that reflection cannot account for the magnitudes that Shropshire observed for the differential growth responses in air. He reasoned that surface reflections are compensated quantitatively by multiple internal reflections within the sph. Jaffe's analysis, however, is valid only for the limiting cases of zero and 100% internal light attenuation. Interpolating linearly between these limiting values, Jaffe concluded that reflection can only explain a 1.6% difference in effectiveness of two polarized beams.

The validity of this linear interpolation, however, is questionable since it is making a dubious assumption about the linearity of the system. The problem is better solved experimentally by utilizing mutants of Phycomyces aberrant in carotene production. These produce sporangiophores which differ markedly from the wild type in their optical density when grown on various media. The carA5 (C2) and carB10 (C5)

mutants (Meissner and Delbruck, 1968; Ootaki et al., 1973) display a much reduced optical attenuation, approaching the limiting case of the transparent cylinder. carR21 (C9) (Meissner and Delbruck, 1968) has intermediate value of attenuation, but greater than wild type. Finally, a newly selected mutant, car-41 (C158), has a very large optical attenuation. Using these mutants, Jaffe's interpolation can be checked with a physiological range of attenuations for which the reflection hypothesis would predict a number of different values.

The existence of oriented screening pigments and structures within the cell could also give rise to the polarized light effect in Phycomyces. This can be checked by microspectrophotometric measurements of the in vivo optical attenuation of polarized light.

If the polarized light effect is due to the orientation and dichroism of the Phycomyces visual pigment, then the maximum response need not be for light polarized transversely. It should be possible to measure the angle of orientation of the absorption transition moments by polarizing the stimulating light at angles away from the longitudinal or transverse directions.

Absorption by linearly dichroic oscillators is proportional to $\cos^2 \alpha$, where α is the angle between the \vec{E} -vector and the absorption transition moment. A periodic variation in response, related to this function, should be observed when sweeping through various angles that \vec{E} makes relative to the sph axis.

This thesis discusses the measurement of the differential growth response of the wild type and of the mutant strains C2, C5, C9, and C158 of Phycomyces to the longitudinal and transverse orientations of

the \vec{E} -vector of linearly polarized light. It describes measurements of the in vivo optical attenuation of polarized light of wavelengths 306 nm, 320 nm, 446 nm, and 486 nm of the above strains. It concludes that the visual pigment is oriented and dichroic and details the measurement of the average orientations of the 280 nm, 456 nm, and 486 absorption oscillators of the visual pigment.

MATERIALS AND METHODS

Strains

Five strains of Phycomyces blakesleeanus were used in this study and are listed in Table I. The mutants differ from the wild type in β -carotene synthesis. C2 and C5 are colorless, C9 is red, producing lycopene instead of β -carotene, and C158 is "superyellow", producing a high concentration of β -carotene (Hsu, 1973).

Growth Media

The media used are listed in Table II.

Culture Conditions

Spores of all five strains were diluted to 100/ml of Hershey broth, heat shocked for 15 min at 48^o C, and inoculated into 3 cm high, 1 cm diameter vials (4.5 x 1.4 cm vials for C158), containing 2 ml of various media. Wild type was grown on PDA and PDAY, C2 on LAC, C5 on PDA, C9 on PDAY, and C158 on GALY media. These were kept in closed glass jars containing 20 vials at 20^o C in room light of intensity 20 μ watt/cm². When the first spps appeared the jars were opened and placed in growth chambers. Temperature was 22^o C, the relative humidity 50-80%, and the illumination was 4-5 μ watts/cm² from overhead tungsten lamps.

The spps were harvested twice a day. The second through seventh crops of spps, lengths 2.0-4.0 cm (wild type, C2, C5, C9) and 4.0-5.0 cm (C158), were used for all measurements.

Light Sources

Spps were illuminated by a horizontal, collimated beam of light

TABLE I

STRAINS OF PHYCOMYCES BLAKESLEEANUS USED IN THIS WORK

Strains C2, C5, C9, C158 were derived from spores of NRRL 1555 mutagenized by nitrosoguanidine as described in Heisenberg and Cerda-Olmedo (1968).

Strain	Genotype	Phenotype
NRRL 1555	(-)	Wild type
C2	<u>carA5</u> (-)	Albino, < 1% normal β -carotene, normal sensory responses
C5	<u>carB10</u> (-)	Albino, < .1% normal β -carotene, normal phototropic threshold
C9	<u>carR21</u> (-)	Red, accumulates lycopene, normal phototropic threshold
C158	<u>car-41</u> (-)	Super yellow, accumulates β -carotene, negative phototropism, normal threshold, normal growth response

TABLE II
GROWTH MEDIA

Hershey Broth

Nutrient Broth	8 g (Difco Lab, Detroit, MI)
Bacto Peptone	5 g (Difco Lab)
NaCl	5 g
Glucose	11 g
pH 7.2-7.4 Distilled H ₂ O	1 l

PDA - Potato Dextrose Agar (4%)

Potato Dextrose Agar	40 g/l (Difco Lab)
.05% Thiamine - HCl	1 ml
Distilled H ₂ O	1 l

PDAY - Potato Dextrose Agar Plus Yeast

PDA	1 l
Yeast Extract	1 g (Difco Lab)

LAC - Lactate Medium

* Agar	10 g
Ammonium Lactate	5 g
Magnesium Lactate	4 g
KH ₂ PO ₄	3 g
MgSO ₄ · 7H ₂ O	1 g
MnSO ₄ · H ₂ O	.2 g
.05% Thiamine - HCl	.1 ml
Distilled H ₂ O	1 l

GALY - Glucose Asparagine Leucine Plus Yeast

* Agar	10 g (Difco Lab)	
* Glucose	30 g	
L-Asparagine	2 g	
L-Leucine	5 g	
MgSO ₄ · 7H ₂ O	.5 g	
KH ₂ PO ₄	1.5 g	
.05% Thiamine - HCl	.5 ml	
* Yeast Extract	1 g	* (solutions autoclaved separately)
Distilled H ₂ O	1 l	

of desired spectral composition and polarization. For experiments utilizing visible light, a simple single lens projector with a tungsten or tungsten halogen lamp (Sylvania Electric Products, Inc., Danvers, Mass.) served as the source. The lamp was powered by a voltage stabilizer (Raytheon Corp., Waltham, Mass.) and potentiometer (Superior Electric Co., Bristol, Conn., Powerstat) or a regulated D. C. power supply (Lambda Electronics Corp., Melville, N. Y., C-880M). The beam was filtered first by a heat absorbing filter (Rolyn Optics Corp., Arcadia, Ca., KG3, 5 mm) and either a broad band blue color filter (Corning Glass Works, Corning, N. Y., 5-61, 5 mm), a 455.5 nm interference filter (Ealing Optical Services, Cambridge, Mass., HBW = 10 nm) or a 486 nm interference filter (Bausch & Lomb Corp., Rochester, N. Y., HBW = 7 nm).

The ultraviolet source was a deuterium lamp (Shoeffel Instrument Corp., Westwood, N. J., Model L-201) powered by a 30 watt DC regulated power supply (Shoeffel, Model LPS-201). The beam was collimated by a quartz lens and passed through a 280 nm interference filter (Ealing Optical Services, HBW = 10 nm).

Polarization

The light was polarized by dichroic polarizing films (Polacoat, Inc., Blueash, Ohio, PL40 for 280 nm light; Polaroid Corporation, Cambridge, Mass., HN22 for broad band blue light, HN38 for 455.5 nm and 486 nm light). The polarizer was mounted on an automatic device which rotated the filter 90° every 5 minutes. The initial orientation of the polarizer could be changed so that any angle of \vec{E} relative to the sph axis could be obtained.

Intensity

The intensities of the polarized stimulus beams were independent of \vec{E} -vector angle for the monochromatic sources. The tungsten source used for the early broad band blue experiments on the wild type and C5 strains emitted light which was 2.5% more intense when polarized transversely than when polarized longitudinally. In these experiments, the results were adjusted to compensate for this systematic error. In subsequent investigations, an isotropic source was used.

The spectral composition of the light was unaffected by changes in polarization and intensity. Intensities were monitored throughout each experiment and were well regulated showing a maximum drift of $\pm 5\%$. The absolute intensities of the different lights used were: 1.6-1.9 $\mu\text{watt}/\text{cm}^2$ for broad band blue, 1.3 $\mu\text{watt}/\text{cm}^2$ for 486 nm, 1.2 $\mu\text{watt}/\text{cm}^2$ for 456 nm, and 0.6 $\mu\text{watt}/\text{cm}^2$ for 280 nm light. These intensities were measured with a photodiode (United Detector Technology, Santa Monica, Ca., UDT PIN 5) and electrometer (Princeton Applied Research Inc., Princeton, N.J., Model 130) and with a calibrated 935 phototube (RCA Corp., Lancaster, Pa., Type 935) and electrometer (Eldorado Electronics, Inc., Concord, Ca., Model 201). The beams were uniform in cross section to 2% for an area of 7 mm in diameter for the 280 nm light and 2 cm for the tungsten light. Spghs were always kept within these uniform areas.

Physiological Experiments

Phycomyces spghs respond to changes in light intensity by changing their growth rate. This is called the light growth response (Bergman et al., 1969, p. 119). A periodic 5 minute (min) step up, 5 min step

down intensity change produces a sinusoidal change in growth rate with a 10 min period. Because the growth response has a latency, the sinusoidal response is phase shifted so that the maximum growth rate occurs halfway through the low intensity interval and the minimum rate, halfway through the high intensity interval (Fig. 2b). If the stimulating light program consists of constant intensity but periodic changes in polarization from 5 min transverse to 5 min longitudinal, a similar response is observed. The maximum of the response occurs during the longitudinal interval (Fig. 3a). In both cases the growth rate variation expresses a difference in intensity perceived by the spph. Comparing this intensity difference for various strains gives a measure of their relative response to changes in the polarization of light.

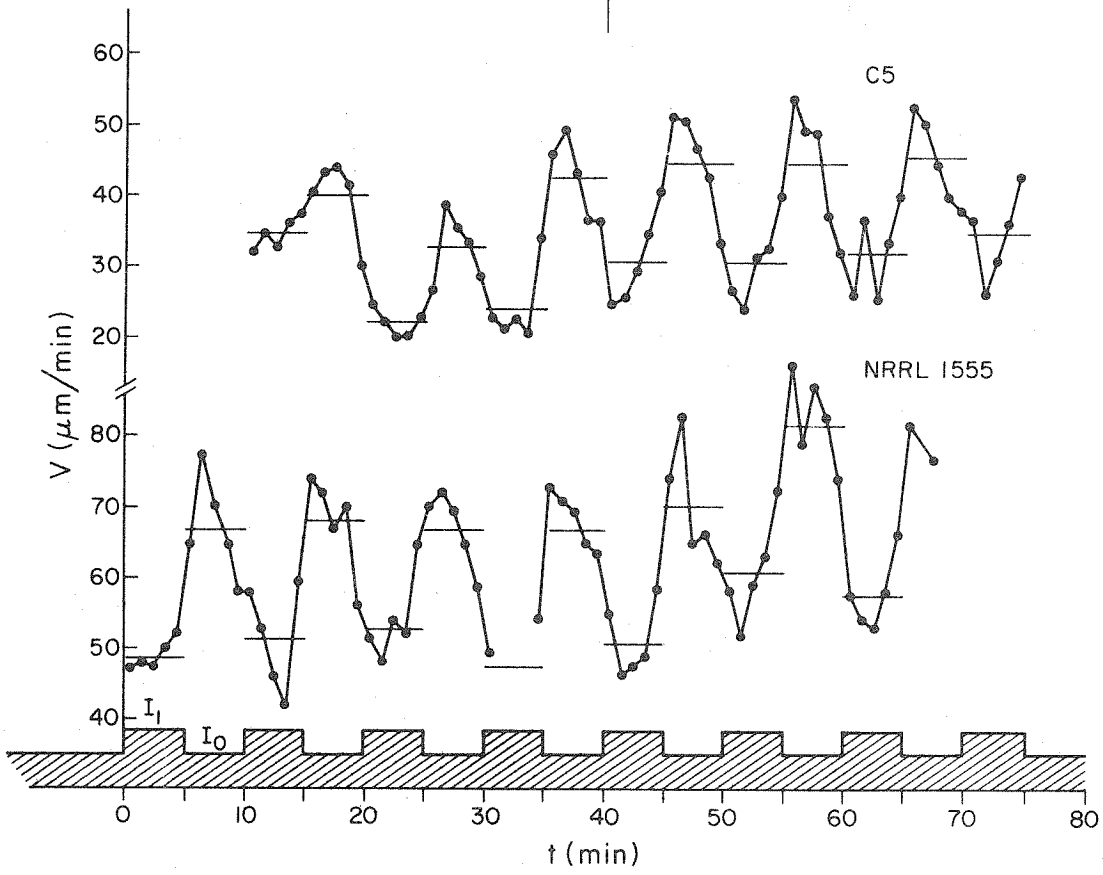
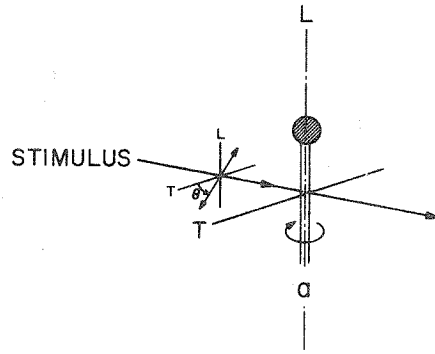
A vertical spph was selected and fastened to the side of the vial with tape or silicone grease approximately 1 cm below the sporangium. The vial was placed on a platform rotated at 2 rpm and mounted on a micro-manipulator permitting fine motions in three mutually perpendicular directions. By adjustments with two screws on the platform, the sporangium could be centered on the axis of rotation. This arrangement permitted spph position measurement, symmetrical illumination, and vertical growth.

The spph was centered in the beam and after adapting to the light program for one hour, the position of the top of the sporangium was measured to $\pm 0.7 \mu\text{m}$ using a measuring microscope fitted with a Filar micrometer (Gaertner Scientific Corp., Chicago, Ill.). This was done every 5 min at the moment the polarizer ceased rotating. Immediately following this, the angular deviation of the spph from the vertical was

Figure 2. Illumination arrangement and growth responses.

a. Direction of irradiation and polarization of the stimulating light. The longitudinal and transverse direction is indicated by T and L respectively. The angle of \vec{E} relative to the transverse axis is θ . The sporangiophore is rotated in the beam at 2 rpm for symmetrical stimulation.

b. Growth rate, V, in response to a periodic light program of alternating intensities. Flux levels are $I_0 = 1.3 \mu \text{ watt/cm}^2$ and $I_1 = 2 I_0$. Growth is measured in 1 min intervals. The response of two strains is shown: C5 above, wild type below. Horizontal bars indicate 5 min average growth rate during I_0 and I_1 periods. The light program is indicated by the hatched area. The height of this area is proportional to the intensity.

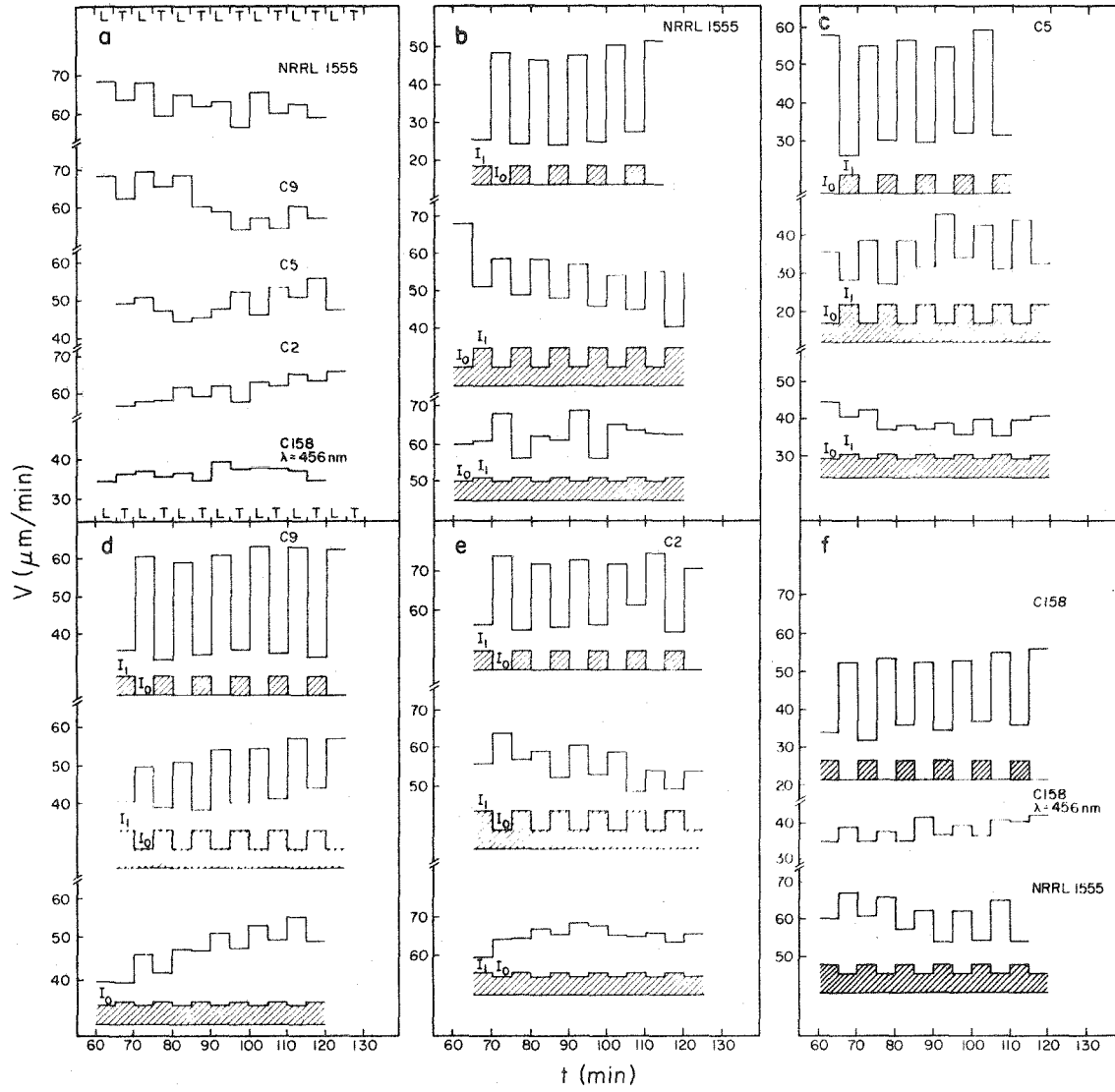


b

Figure 3. Growth responses to polarized light and intensity alternations.

a. Growth rate of five strains of Phycomyces in response to a periodic light program of alternating orientations of the \vec{E} -vector of polarized blue light. \vec{E} orientations are longitudinal (L) and transverse (T). Intensity about $1.8 \mu\text{watt}/\text{cm}^2$.

b-f. Five minute average growth rate in response to a periodic light program of alternating intensities I_1, I_0 for 5 strains of Phycomyces. Light programs are indicated by hatched areas. $(I_1 - I_0)/(I_1 + I_0) = 1.00$ for upper curve, 0.33 for middle curve, 0.10 for lower curve. For C158, lower two curves are a comparison with the wild type of a response to $(I_1 - I_0)/(I_1 + I_0) = 0.2$.



measured using a goniometer accurate to $\pm 2^\circ$. This never exceeded 30° and was used for correcting the measured growth for its cosine error in the field of the microscope. The field of view was illuminated with physiologically inactive red light (Corning Glass Works, Corning, N. Y., Type 2-59). An enclosure built around the apparatus kept the temperature constant to 1% and humidity constant to 5%. The temperature for the entire experimental series was kept at $20^\circ \pm 2^\circ\text{C}$. Fig. 4 shows the experimental arrangement.

The total growth during a number of periods of one \vec{E} orientation was compared with that during the orthogonal orientation thus giving a measurement of the differential growth response to polarized light. This response was calibrated in terms of an intensity difference of unpolarized light as perceived by the sph by alternating between two intensities every 5 min. The base level intensity was kept constant at 1.6 or 1.9 $\mu\text{watt}/\text{cm}^2$. Alternating the voltage between two levels every 5 min produced the desired intensity change. The maximum difference produced was 136% with a negligible change in spectral composition. The ultraviolet calibration was done using neutral density filters (Ealing Optical Services).

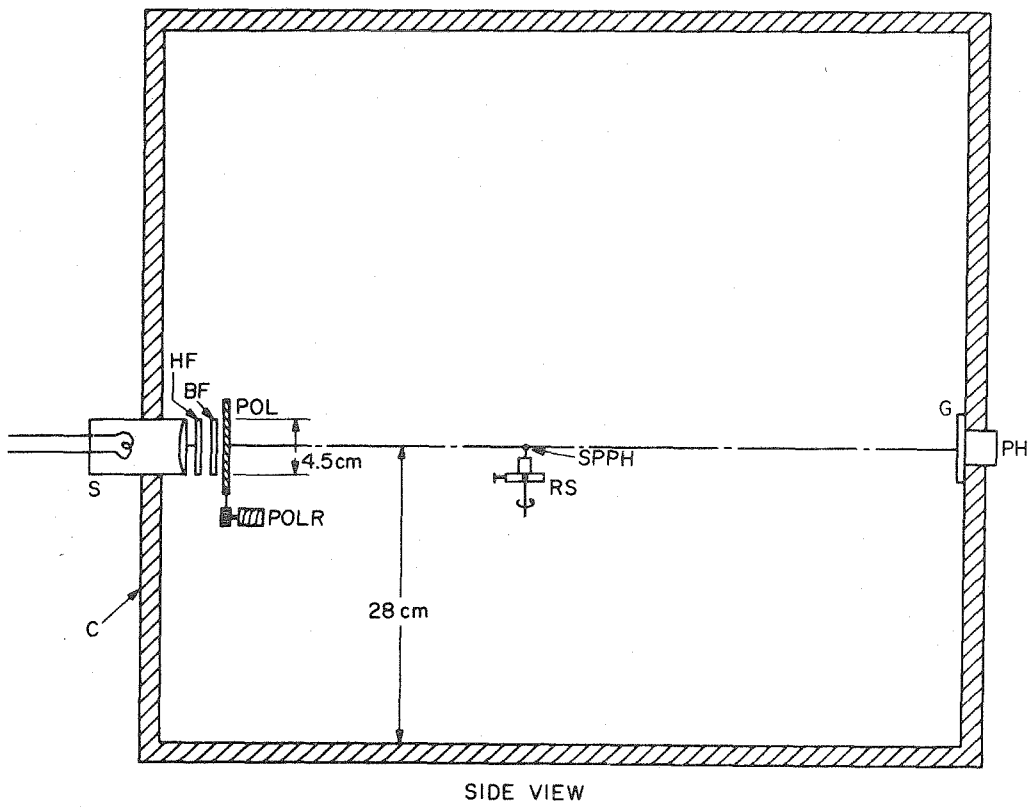
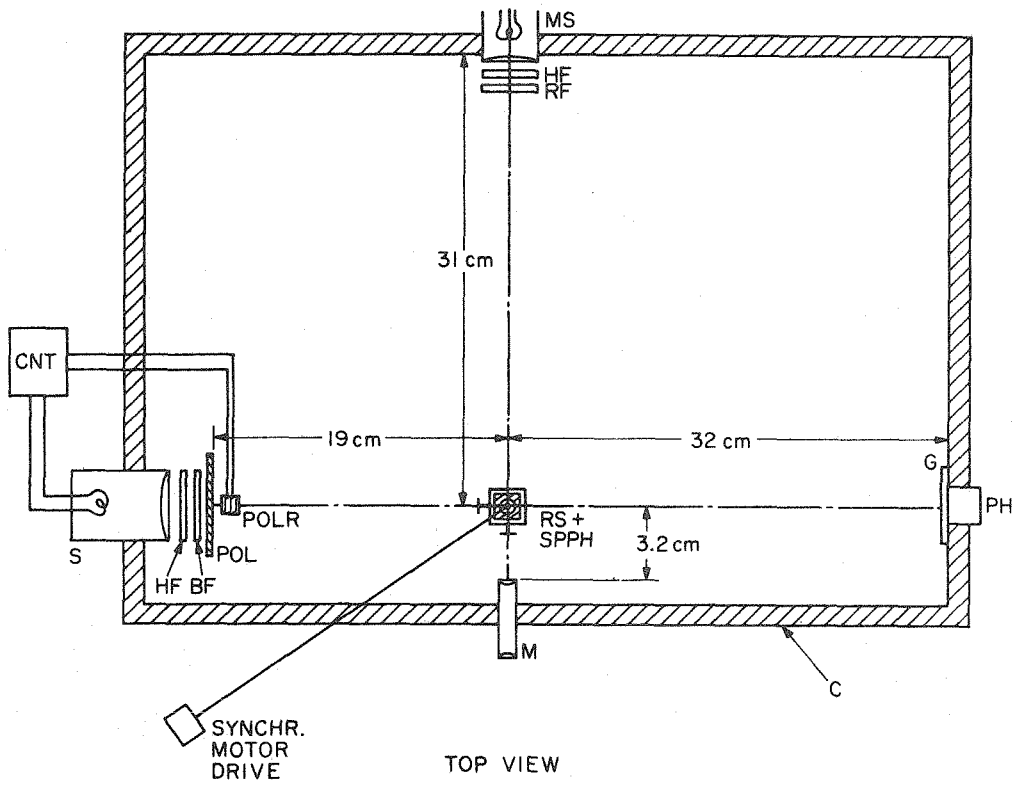
The growth during the high intensity period was compared to that during the low intensity period and the response plotted as a function of intensity change. This gave a measure of the sensitivity of each strain to intensity differences and a way to compare the different strains' sensitivities to polarized light.

Microspectrophotometry

In vivo absorbance measurements of the growing zones of live

Figure 4. Apparatus for light programs.

Legend: BF, blue filter; C, chamber with controlled temperature; CNT, polarizer rotation control or intensity switching control; G, glass plate; HF, heat absorbing filter; M, microscope; MS, microscope source; PH, photometer; POL, polaroid; POLR, polaroid rotator; RF, red filter; RS, rotating stage; S, stimulus source; SPPH, sporangio-
phore.



sporangiohores were made with a Cary Model 15 spectrophotometer (Applied Physics Corp., Monrovia, Ca.) with a microscope attachment as described by Zankel et al. (1967). This attachment was improved for measurements of absorption anisotropy and ultraviolet absorption. The modifications included exchange of objectives for ultraviolet transmitting glycerine immersion types (Carl Zeiss Corp., New York, N. Y.; 100X, 1.25 NA; 32 X, 0.40 NA ultrafluor) and rotatable Glan Thompson polarizing prisms (Karl Lambrecht Corp., Chicago, Ill.) mounted in the reference and sample beams.

The absorption spectra of C2, C9, and C158 as well as their absorbance differences between longitudinally and transversely polarized light (ΔOD_{L-T}) at 450 nm and 500 nm were measured on the unmodified attachment. Specimens were prepared in the same way as described by Zankel et al. ΔOD_{L-T} was measured for both the spph and the blank slide adjacent to the spph and then subtracted. The sample beam was polarized using an HN38 polaroid (Polaroid Corp.).

Absorption anisotropy was measured on the improved instrument at 455 nm and 486 nm for C158, and 306 nm and 320 nm for the wild type. The purpose of measurements at 306 nm and 320 nm was to obtain an extrapolated value of the anisotropy at 280 nm, since the polarizing prisms did not transmit sufficient light for measurement at this wavelength. Both reference and sample polarizers were rotated simultaneously through 180° starting from an orientation perpendicular to the spph axis. The changes in absorbance were recorded in 15° increments. The same was done for the adjacent blank region of the slide. The results were sub-

tracted to remove polarization artifacts of the instrument and mount.

The spectra including the ultraviolet region were measured using the modified attachment with the specimen mounted in distilled water, sandwiched between two quartz cover slips (Ammersil Inc., Hillside, N. J.).

RESULTS

A. Differential Growth Response of Wild Type and Mutants to Longitudinally and Transversely Polarized Broad Band Blue Light

Each of the strains showed responses typical of the alternating light intensity programs employed by Delbrück and Shropshire (1960). Let L and T denote longitudinally and transversely polarized light respectively. Fig. 2a shows the average growth rate during each 5 minute, T and L, half cycle for a typical spph of each strain. Figs. 3b-f show similar graphs for light programs in which the intensity was alternated between two levels, $I_1 > I_0$, differing by 20% ($[I_1 - I_0] / [I_1 + I_0] \sim 0.1$). Both sets appear very similar in both the magnitude and variability of the response. For a comparison, the response to an intensity program, with $I_1 = 2I_0$ and with $I_0 = 0$, is shown in Fig. 2b-f. The responses in this case are much larger and show a much smaller relative variation. Because of the small size of the polarized light response, its quantitative estimation required observation of several spph (4-13) for many 10 min cycles (34-123).

From the measurements of total growth during each T and L half cycle, the average growth rate for all T periods and all L periods was computed for each spph observed. One-half the difference of the rates during the two periods is called the amplitude of growth rate variation. The quotient of this quantity and the average growth rate is called the relative amplitude of growth rate variation, r . The average, \bar{r} , was calculated for several spphs by weighting each r by its

variance, σ (Appendix I). Thus, spphs observed for many cycles showing little variation, are much more influential in the calculation of the mean than noisy spphs observed for few cycles. This procedure assumes there is no correlation between sph noise and its ability to respond. By comparing r from groups with large and small σ 's, it is easily seen that the assumption is a valid one. The ratio of the averages of the two groups is 0.9 ± 0.4 . Table III gives \bar{r} for each strain used.

For the early broad band blue experiments in the wild type and C5 strains, it was noticed that each time the polaroid rotated, the sph vibrated, suggesting that it was perhaps mechanically stimulated. Experimental runs, called vibration checks, were made on C5 and wild type sph in which the polarizer was absent from the mount while the apparatus continued to function and all readings were taken as though a polarization experiment were in progress. A similar quantity for the differential growth response to this stimulus was also computed and used to correct for these vibrations. This rotator was replaced by one which did not produce vibrations in subsequent experiments.

The quantities in parentheses in Table III refer to those measured in early experiments which have been corrected for intrinsic polarization of the source ($I_T/I_L = 1.025$) and mechanical vibrations produced by the rotator (Wild type $\bar{r}_{\text{vibr.}} = 1.4 \pm 0.5\%$, C5 $\bar{r}_{\text{vibr.}} = 1.0 \pm 0.5\%$). Agreement with the values above then indicates that these corrections were reasonable.

These values are to be compared with respect to the sensitivity

TABLE III

AVERAGE RESPONSES OF 5 STRAINS TO ALTERNATING 5 MINUTE PERIODS
OF LONGITUDINALLY AND TRANSVERSELY POLARIZED BLUE LIGHT

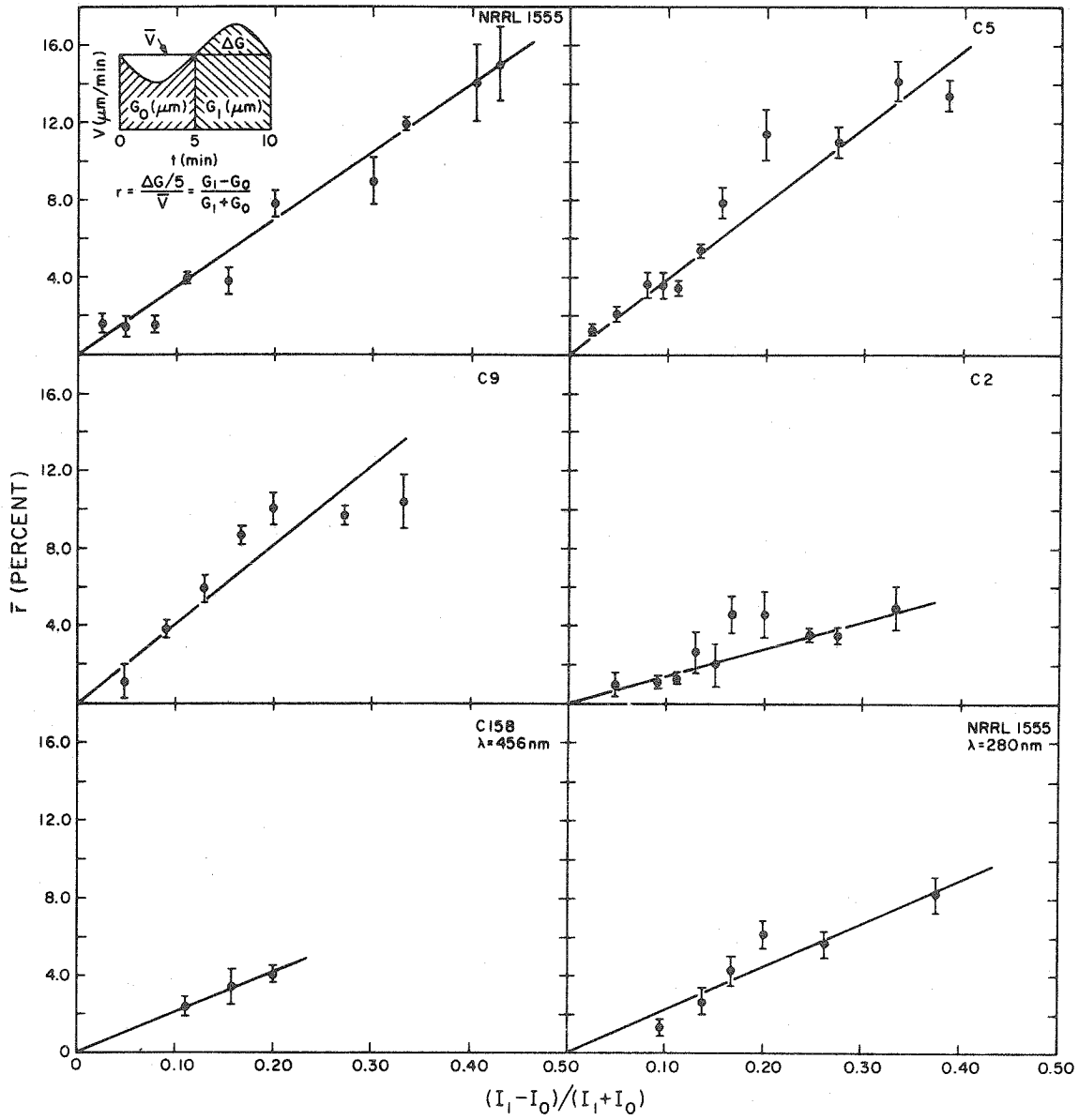
Strain	$\bar{r} \times 100$ %	Number sphs, cycles observed	$(\Delta I/I_0)_{eq} \times 100$ %	Number sphs, cycles observed for response curves
NRRL 1555	3.5 ± 0.7 (3.8 ± 0.7)	4, 34 (6, 100)	22 ± 5 (24 ± 5)	33, 330 (33, 330)
C5	3.6 ± 0.2 (3.6 ± 0.7)	5, 39 (7, 23)	20 ± 2 (20 ± 4)	44, 417 (44, 417)
C2	1.9 ± 0.4	12, 71	32 ± 7	53, 328
C9	3.8 ± 0.3	13, 77	21 ± 2	39, 232
CL58 $\lambda = 456 \text{ nm}$	1.3 ± 0.3	32, 260	14 ± 5	12, 96

of each strain to light intensity differences. An analogous quantity, \bar{r}' , was computed for the response of the sph to alternating 5 min intervals of light at intensities I_1 and I_0 . Fig. 5 shows a plot of \bar{r}' as a function of the differential intensity change $(I_1 - I_0)/(I_1 + I_0)$, for each strain. This quantity can also be expressed as $[1 + 2 (\frac{I_0}{\Delta I})]^{-1}$, where $\Delta I/I_0 \times 100$ is just the percent change in light intensity. The regions where \bar{r}' appears to be linear depend on the strain and were selected by inspection. Straight lines were fitted to the data in these regions by the method of least squares.

Additional experiments with broad band blue light at a differential intensity = 1.0 (i.e. $I_0 = 0$) produced the maximum response obtained for all the strains (Fig. 3). \bar{r}' for these experiments was always smaller than the extrapolated values from the curves in Fig. 5, showing that the response begins to saturate. Since the value of the differential intensity corresponding to the polarized light response was small, approximately .1, the use of only the small values of \bar{r}' and the assumption of linearity seems justified.

Thus, if a sph sees a light intensity difference when it is exposed to alternations of \bar{E} , \bar{r} can be made equivalent to an \bar{r}' and a corresponding $\Delta I/I_0$ can be assigned to it. This is the equivalent intensity difference perceived by the sph when the polarization is changed from T to L. It is given alongside \bar{r} in Table III. The standard deviation of this quantity was determined by the propagation of the variance of \bar{r} in the calculation of $\Delta I/I_0$ from the least squares parameters of the response curves.

Figure 5. Growth response versus intensity differentials. \bar{r} is the relative amplitude of the growth rate change during a periodic stimulus program consisting of 5 min of intensity I_0 alternating with 5 min of I_1 . It is taken as the total growth, G_0 in μm , for all the I_0 periods, minus growth, G_1 , for all the I_1 periods divided by the total growth $G_1 + G_0$. This quantity is the ratio of the amplitude of the growth rate change ($\Delta G/5$) and the average growth rate (\bar{V}) during the entire run. The mean for several sporangiophores, \bar{r} , is plotted as a function of $(I_1 - I_0)/(I_1 + I_0)$. The strain is indicated in the upper right of each graph along with the wavelength of light if not broad band blue.



In summary, all four strains are 20% more sensitive to transversely rather than longitudinally polarized light. The transparent strains do not show a smaller effect and the optically dense strains show no larger effect.

B. Microspectrophotometry

The visible absorption spectrum of wild type, C5, C2, and C9 are given on p. 135 in Bergman et al. (1969). Fig. 6 shows that of C158 and wild type. It also shows the U.V. absorption spectrum of the wild type. Both strains show a very high attenuation of light at specific wavelengths. This property has been used in section C. C9 and C2 were grown under different conditions than listed in Bergman et al. and consequently their spectra are shifted in the vertical direction slightly. The absorbance values at 450 and 500 nm for all the strains are given in Table IV.

C2, C9, C158 and the wild type were investigated for absorption anisotropy with respect to polarized light. Table V gives the optical density differences between longitudinally and transversely polarized light, $\overline{\Delta OD}_{L-T}$, as well as the maximum optical density difference $\overline{\Delta OD}_{MAX}$ encountered in measuring OD as a function \vec{E} -vector angle. In all cases, the anisotropy was very small, at most $.014 \pm .009$.

C. \vec{E} -Vector Angle for Maximum Response at 280 nm, 456 nm, and 486 nm

The cylindrical symmetry of the sph requires that the orientation of the receptor dipoles be antisymmetric with respect to reflection through the plane determined by the sph's diameter and longitudinal axis. Thus, dipoles in the proximal half of the cell, whose

TABLE IV

IN VIVO ABSORBANCE VALUES AT 500 nm AND 450 nm FOR 5 STRAINS

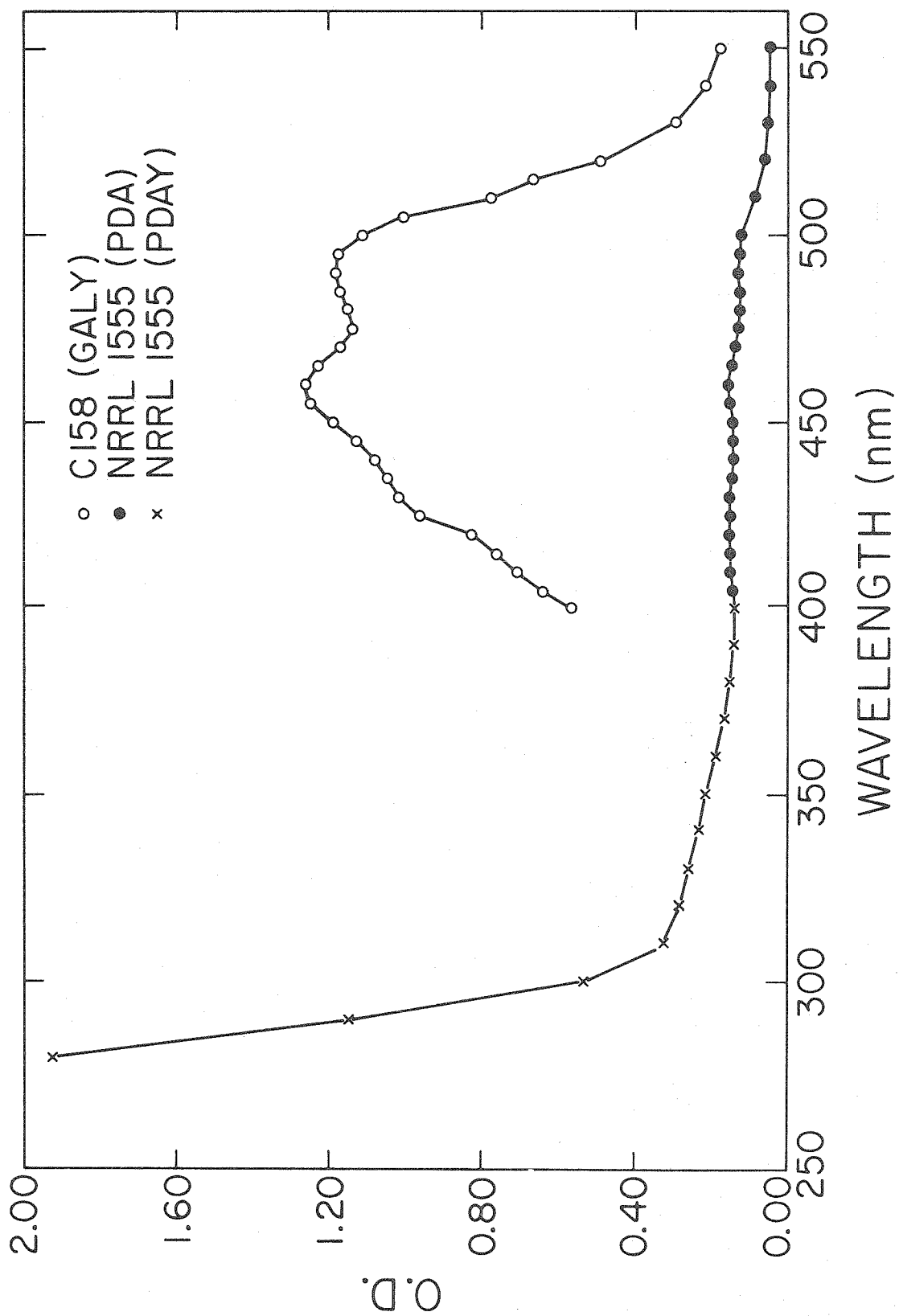
Strain	Growth medium	OD ₄₅₀	OD ₅₀₀
NRRL 1555	PDA	.14	.12
C5	PDA (from Bergman et al., 1969)	.05	.04
C2	LAC	.06	.04
C9	PDAY	.16	.16
C158	GALY	1.19	1.11

Experimental precision = \pm 0.01.

TABLE V
POLARIZED LIGHT ABSORPTION ANISOTROPY

Strain	Growth medium	λ nm	$\overline{\Delta OD}_{L-T} \times 10^2$	$\overline{\Delta OD}_{MAX} \times 10^2$
NRRL 1555	PDAY	306	2 ± 1	2 ± 1
	PDAY	320	$0.0 \pm .4$	$1.5 \pm .7$
	PDA	463	0 ± 1	-
C2	LAC	450	$1.2 \pm .5$	-
	LAC	463	$0.6 \pm .8$	-
	LAC	500	$0.9 \pm .3$	-
C9	PDAY	450	$0.3 \pm .2$	-
	PDAY	500	$0.6 \pm .1$	-
C158	GALY	455	$0.9 \pm .7$	$1.4 \pm .9$
	GALY	486	$0.2 \pm .4$	$0.8 \pm .5$

Figure 6. Sporangiphore absorption spectra. Visible absorption spectra of C158 grown on GALY medium, wild type grown on PDA. Optical density (OD) is plotted as a function of wavelength.



projections in the T-L plane (Fig. 2a) are oriented at an angle, α , to the transverse axis, will be matched by an equal number of dipoles in the distal half, oriented at an angle $-\alpha$. Intuitively, this means that absorption can be maximum only at values of θ equal to 0° or 90° ; that is, when E bisects the angle 2α between the two sets of dipoles. For $\alpha < 45^\circ$ absorption will be maximum at $\theta=0^\circ$, and for $\alpha > 45^\circ$ it will be maximum at $\theta=90^\circ$. Quantitatively, the absorption is proportional to $\cos^2(\theta-\alpha) + \cos^2(\theta+\alpha)$, which has extrema at $n\pi/2$ where $n=0,1,2,\dots$. Thus regardless of what α is, the sph will always show a maximum response at $\theta = 0^\circ$ or 90° .

This difficulty was circumvented by choosing wavelengths and strains displaying high optical densities. At 280 nm the absorbance of wild type is 1.9 ± 0.1 ; at 456 nm and 486 nm the absorbance of C158 is 1.3 ± 0.2 and 1.2 ± 0.2 respectively. For these high absorbancies, the influence of the distal region becomes negligible and \bar{r} will show a dependence on θ , indicative of the average orientation.

Let $\bar{\alpha}$ be the average α for all the receptor absorption dipoles in the proximal half of the sph. Receptor absorption for light polarized at angles θ and $\theta+90^\circ$ to the transverse axis will be proportional to $I_1 = \cos^2(\theta-\bar{\alpha})$ and $I_0 = \sin^2(\theta-\bar{\alpha})$ respectively. Since r' is proportional to $(I_1 - I_0)/(I_1 + I_0)$ in the intensity cycling experiments, the corresponding r in these experiments will be proportional to $\cos 2(\theta-\bar{\alpha})$. This differential absorption, D , will be maximum when $\theta \equiv \theta_{\max} = \bar{\alpha}$, have the period π , and possess the property: $D(\theta) = -D(\theta+90)$. These properties are also common to r , a measure of the

differential growth response.

r was measured for light programs consisting of 5 min alternations between light polarized at the angle θ and the angle $\theta + 90^\circ$. For each θ , 5 spps were observed over a total of approximately 45 cycles. θ took on values from 0° to 75° in 15° increments. Thus, six values of \bar{r} were obtained corresponding to the six angles.

These six values were plotted against θ . The function $r_{\max} \cos 2(\theta - \theta_{\max})$ was least squares fitted to the data. From this fitted curve θ_{\max} , the angle of maximum response, and r_{\max} , the maximum differential growth response, were obtained. These results are shown in Fig. 7 and summarized in Table VI.

In all the physiological experiments, the reading errors and errors due to fluctuations in growth rate were minimized by running experiments over many cycles. The largest error came from interspecimen variation. This variation, however, can be tolerated in light of the conclusions made.

The intensity difference experiments showed consistency in the response curves. " χ^2 ", the sum of the squares of deviations of the data points from the least square line, was close to one for all strains, indicating a good fit.

Other errors were relatively small and, therefore, did not interfere with the spps response or its measurement.

The experiments were not all done at the same intensity levels. This fact probably has little significance. The response is a function of the quotient of (intensity x time) and adaptation level (Bergman et al., 1969) and the spps were fully adapted to the intensity

Figure 7. Polarized light responses versus θ , at high optical density. Relative amplitude of growth rate change as a function of \vec{E} vector angle relative to the transverse axis of the sporangiophore. The light program consists of a periodic alternation between \vec{E} oriented at θ and $\theta + 90^\circ$. $\bar{r}_{\max} \cos 2(\theta - \theta_{\max})$ is fitted to the data points by the method of nonlinear least squares. θ_{\max} , the phase angle, is the angle at which maximum response occurs. r_{\max} is the maximum value of the fitted curve. Since an alternation of \vec{E} between $\theta = 0^\circ$ and 90° is the same as an alternation between 90° and 180° , except for phase, $r(90^\circ)$ is shown again as a dotted data point $r(0^\circ) = -r(90^\circ)$.

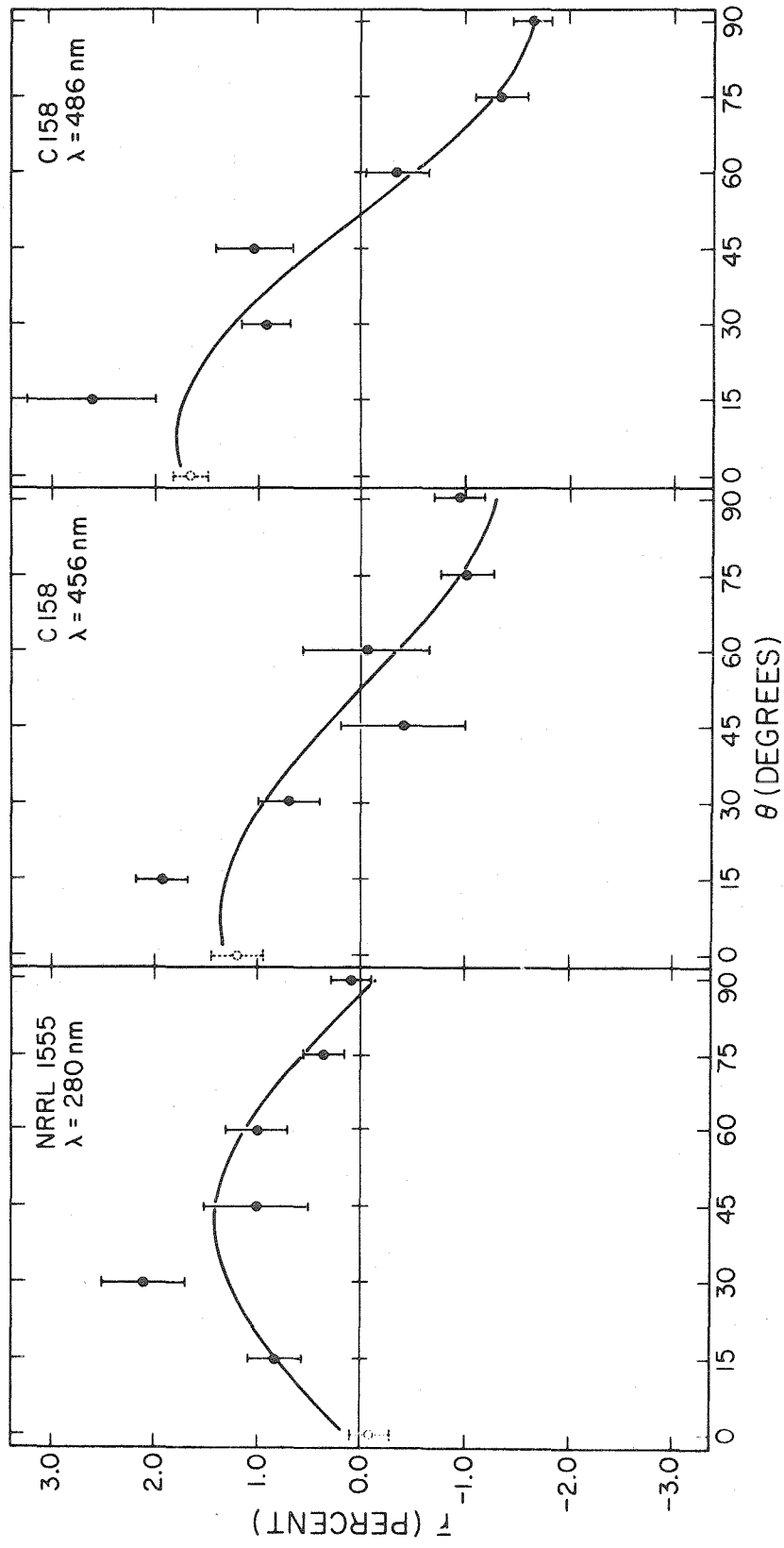


TABLE VI
E VECTOR ANGLES FOR MAXIMUM RESPONSE

Strain	Growth medium	Wavelength λ nm	Transmission T %	Maximum response $\frac{r}{I}$ %	Angle of max. response θ_{max} degrees	Angle of response $(\Delta I/I_0)_{eq}$ %
NRRL 1555	PDAY	280	1.2	1.4 + .3	42 + 4	18 + 8
CI58	GALY	456	5.0	1.3 + .3	7 + 8	14 + 5
CI58	GALY	486	6.3	1.8 + .2	7 + 2	-

levels of the experiments. Consequently, the stimulus produces the same value in any intensity difference or polarization experiment for all intensity levels in the linear range ($.02 - 5 \mu\text{watt}/\text{cm}^2$). The levels utilized never deviated from each other by more than about a factor of 2.

DISCUSSION

The Fresnel Effect

A beam of light impinging on a surface is partially reflected and partially refracted. For a sph, this means that some light gets into the cell and some is reflected away. The quantity of light that is reflected or refracted is determined by the Fresnel reflection coefficients which depend on the refractive indices of the two media, the angle of incidence, and the polarization of the beam. Castle (1934), using these parameters, calculated the absorption of longitudinally and transversely polarized light entering the cell perpendicularly from opposite sides. His graphic integration showed that on the first lap across the sph, the ratio of the light absorbed in the opposite halves of the cell would equal 1 (i.e. phototropic balance) if the longitudinal beam were 20% more intense than the transverse beam. In order to perform the integration, Castle confined the calculation to the limiting case of zero light attenuation but did not consider what would happen on the next lap after the first internal reflection.

Jaffe (1960) took this consideration into account and showed that it should not be neglected. For a homogeneous transparent cylinder, he showed that because of successive internal reflections within the sph, the sum of the light quanta absorbed by a receptor pigment present in low concentration in the series of successive traverses will be independent of reflectivity, for any beam with a given angle of incidence.

Jaffe's proof runs as follows:

- (1) the angle of refraction of a light ray upon entrance

into the cylinder is equal to the angle of reflection at each successive reflection within;

(2) the reflection coefficient for entrance into the cylinder is equal to the reflection coefficient at each successive reflection within;

(3) the sum of the light absorption along the total light path within the cylinder is a geometric series in the reflection coefficients.

Specifically, the total absorption, summed over successive laps, is

$$A = K (1-R) + K (1-R) R + K (1-R) R^2 + \dots = K \text{ for } K \ll 1$$

where A = absorption

K = fraction absorbed during each lap between reflections

R = reflection coefficient.

For small R, the infinite series converges rapidly and can be approximated by the first two terms corresponding to only one internal reflection. This approximation will be adequate to an accuracy of 3% for 85% of light flux normally incident onto the cylinder. Thus, the first internal reflection nearly compensates for the loss by reflection at the first surface. Because each traverse of a light ray, undergoing internal reflections, maintains the same radial position and because the effect of polarization and angle of incidence on the quantity of light entering the cylinder can be expressed in terms of reflection coefficients, Jaffe concludes that the net absorption is independent of these parameters and of the pattern of external illumination.

Jaffe's theorem applies to the case of negligible light losses.

If there is attenuation due to any cause, compensation due to internal

reflections will be incomplete. In wild type *spph* there is 36% light attenuation per lap. Of this attenuation, 18% is due to absorption by β -carotene and the remainder due to scattering. Absorption removes light quanta from the beam while scattering redistributes them. Thus, absorption is more effective than scattering in destroying the compensatory effect of internal reflections. The Jaffe theorem, therefore, cannot be applied directly to the wild type. Jaffe estimated that the effect of different reflections for T and L light would be small, equivalent to a 1.6% intensity difference; and therefore, the Fresnel effect could not account for the large experimental result measured by Shropshire.

In C2 and C5 the optical attenuation is equal to 14% and 12% respectively, due entirely to scattering. Consequently, this attenuation plays a relatively smaller role than it would if it were entirely due to absorption. If reflection losses were the cause of the polarized light effect, then they should be much smaller in the C5 and C2 strains. In contrast, the results show that the polarization effects are as large or larger for C5 and C2 than they are for the wild type.

The average optical density of the red mutant, C9, from 400-500 nm is approximately 20% higher than that of wild type. Consequently, the reflection hypothesis would predict a greater sensitivity to the plane of polarization for C9 than for wild type. In contrast, C9 sees polarization differences equally well as wild type. The same result is obtained for C158, a strain even more optically dense.

In conclusion then, these experiments substantiate Jaffe's contention that the reflection hypothesis cannot be correct. Reflection losses can have only a minute effect on the responses of Phycomyces spphs to polarized light.

Anisotropic Attenuation

We consider next the possibility that the polarized light effect could be a result of anisotropy of the optical attenuation due to screening pigments or to scattering structures.

Back scattering by fibers, having diameters much smaller than the wavelength of light, is greatest for light polarized parallel to the fiber axis (Kerker, 1969). As a consequence, the transversely oriented chitin fibrils (20 nm in diameter; Roelofsen, 1951) spph cell wall would allow more longitudinal rather than transverse light into the cell--a situation producing a polarized light effect opposite in sign to the one measured.

In addition, microspectrophotometric measurements on the growing zones of live spphs have shown that the anisotropy of the attenuation amounted to at most a 3% difference of longitudinally as opposed to transversely polarized light. Clearly, this cannot explain differences of 20-30%.

Oriented Dichroic Receptors

The remaining hypothesis to account for the polarized light effect is the preferential absorption of transversely polarized light by the photoreceptor molecules. This implies that the molecules are linearly dichroic and have an angular distribution of their transition dipoles favoring transverse absorption.

What sort of orientation could produce the observed degree of absorption anisotropy (1.2: 1 for transverse absorption: longitudinal absorption)? In the cylindrical microvilli of crayfish rhabdoms (Waterman et al., 1969), a ratio of 1:2 for transverse: longitudinal absorption has been measured microspectrophotometrically--a bias opposite to that found in *Phycomyces*. This result has been interpreted by postulating receptor dipoles tangent to the cylindrical microvillar surface but randomly oriented in the tangential plane. Such an orientation, implicated in nearly all plants sensitive to polarized blue light, predicts the measured preference for longitudinal absorption. This is perhaps the simplest non-random orientation that can be expected in the cylindrical case.

In *Phycomyces* the transverse component is absorbed more effectively. This means that the dipoles cannot be ordered as in the microvilli, but must have a bias in favor of an equatorial alignment. These possibilities are illustrated in Fig. 8.

Our experiments measuring the polarized light effect for the action peaks at 280, 456, and 486 nm put constraints on the possible average orientation of the transition moments involved. The somewhat involved analysis of the situation will be presented here in outline, with the mathematical details given in Appendix II.

Perfectly Aligned Dipoles

Assume that the photoreceptor absorption transition dipoles can be represented by a vector field:

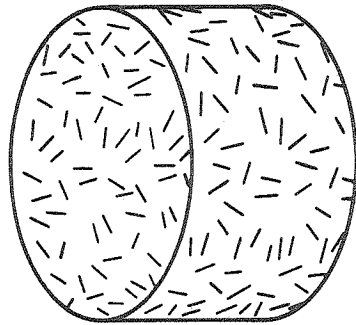
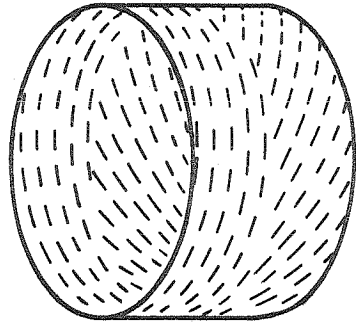
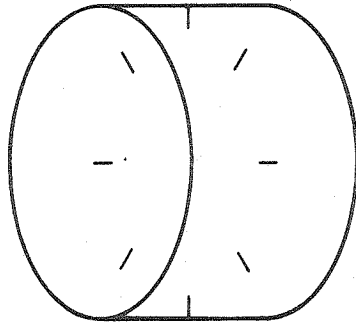
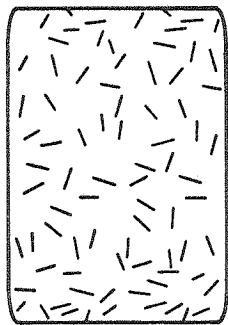
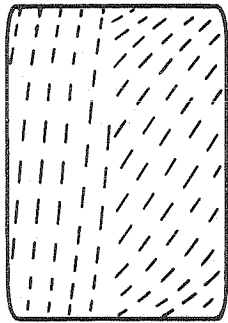
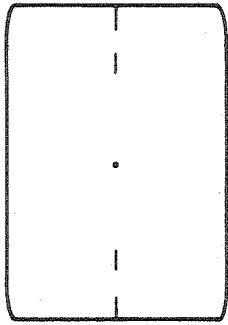
- (1) possessing cylindrical symmetry,

Figure 8. Oblique and normal views of hypothetical receptor transition dipole orientation.

(a) Random orientation in the tangential plane as postulated for the receptor in the microvilli in crayfish rhabdoms. (dichroic ratio 1:2, transverse: longitudinal; Waterman et al., 1969).

(b) Ordered tangential orientation at an angle 5.5° or 33° to the azimuthal axis. Such orientations will produce a maximum dichroism at $\theta = 7^\circ$ and 42° respectively.

(c) Radial orientation. (b) and (c) or a mixture of the two may correspond to the situation in Phycomyces.



(c)

(b)

(a)

- (2) confined to a thin cylindrical shell whose radius equals that of a sph,
- (3) with uniform magnitude corresponding to the magnitude of the absorption transition dipole, and
- (4) with direction corresponding to the orientation of the transition dipole at any point. This orientation is assumed to be perfect and to be characterized by the angles ϕ and χ (Fig. 16).

The relative differential absorption for a pair of test angles, θ and $\theta + 90^\circ$ of the \vec{E} vector, is derived in Appendix IIA, eq. (4). It is given by the expression

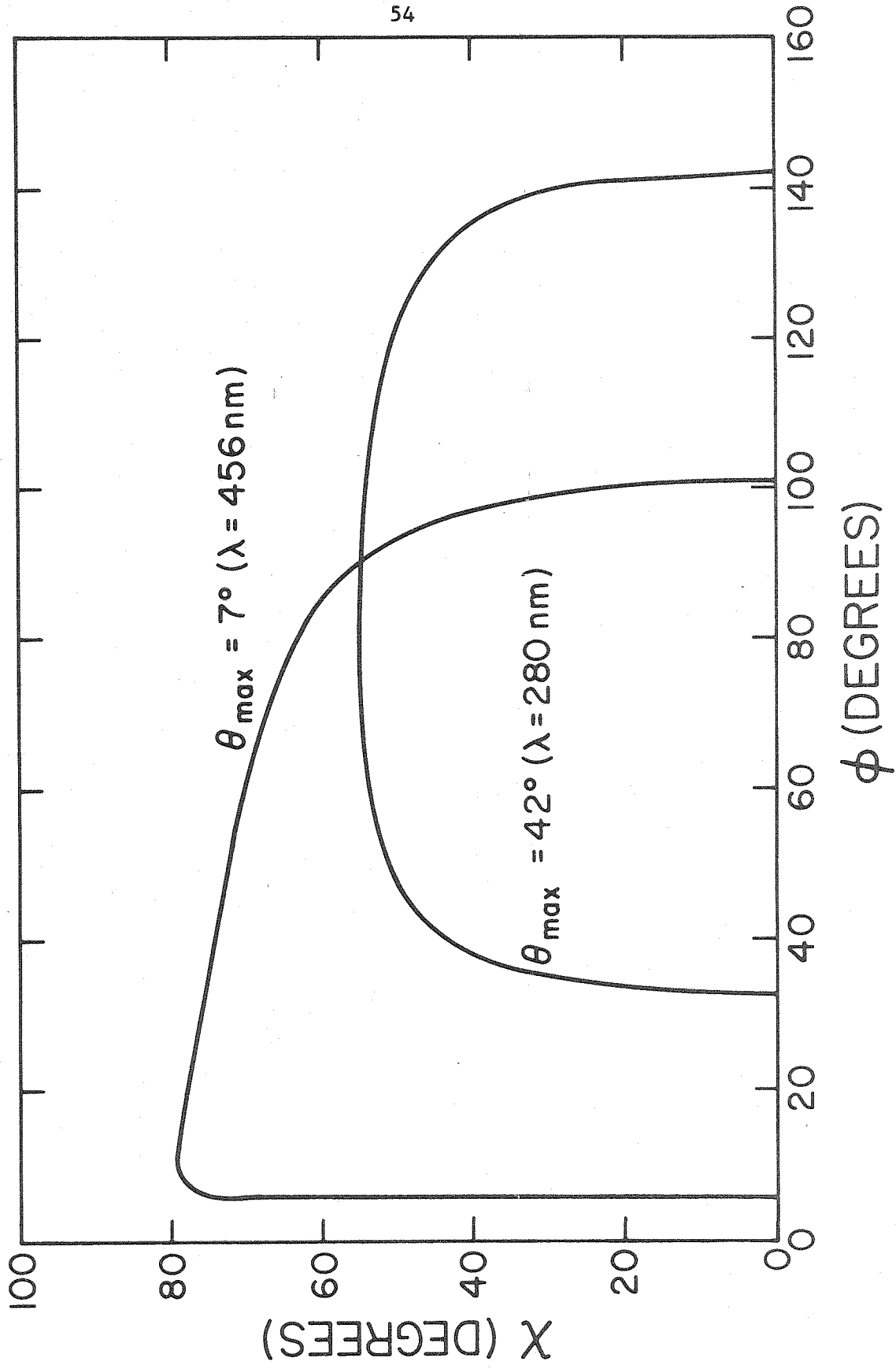
$$D(\theta, \phi, \chi) = \frac{\cos 2\theta (\cos^2 \phi - 2\sin^2 \phi + \tan^2 \chi \sin^2 \phi) + \sin 2\theta \left(\frac{4}{\pi} \sin 2\phi\right)}{1 + \sin^2 \phi + \tan^2 \chi \sin^2 \phi} \quad (\text{IIA4})$$

For a given dipole orientation (ϕ, χ) , D will be maximum ($=D_{\max}$) for a particular θ ($=\theta_{\max}$). θ_{\max} and the angles ϕ, χ are related by equation (6), derived in Appendix IIB.

$$\tan^2 \chi = 2 + \frac{8}{\pi} \cot \phi \cot 2\theta_{\max} - \cot^2 \phi \quad (\text{IIB6})$$

The angles θ_{\max} have been determined for three wavelengths. Each such determination, according to equation (IIB6), establishes a relation between the angles ϕ and χ for the particular dipole involved. In Fig. 9, χ has been plotted as a function of ϕ for $\theta_{\max} = 7^\circ$ and $\theta_{\max} = 42^\circ$, the values observed for 486 and 455 nm, and 280 nm respectively. Since this relation is relatively independent of the assumption of perfect alignment of the dipole field, we have used it in combination with

Figure 9. Possible receptor dipole orientation. χ , the angle between the dipole's projection in the sagittal plane and the longitudinal axis is plotted as a function of ϕ , the angle between the tangential component and azimuthal axis. The two curves correspond to those pairs of values of χ and ϕ suggested by a maximum sensitivity to light polarized at angles $\theta_{\max} = 7^\circ$ (456 nm dipole) and 42° (280 nm dipole) to the transverse axis.



equation (IIA4) to obtain a relation between D_{\max} and ϕ for the three wavelengths, and have plotted this relation in Fig. 10. Similarly, we have used the relations between ϕ and χ , expressed in Fig. 9, to calculate the relative magnitudes of the radial and tangential components for each θ_{\max} and have plotted them in Fig. 11.

Let us first take note that the observed D_{\max} is positive in each case. This implies (Fig. 10) $\phi \leq 90^\circ$, i.e., that the tangential component of the dipole rests in the first and third quadrants. Next, we note from Fig. 9 that χ is large (a strong radial component) unless ϕ is very close to its minimal value. We also note that for $\phi = 90^\circ$ (dipoles confined to the sagittal planes) we have a singular case. For symmetry reasons, θ_{\max} is necessarily 90° (for $\chi < 55^\circ$), or 0° (for $\chi > 55^\circ$). Any other values of θ_{\max} , like those prescribed in constructing Fig. 9, 10, 11, automatically require $D = 0$, i.e., no differential absorption, and therefore no actual maximum of D at the prescribed θ_{\max} .

The measured values of D_{\max} at 456 and 280 nm, inferred from the growth responses are both about 0.06. These values are very low compared to the possible range shown in Fig. 10. Presumably because the assumption of perfect alignment of the dipole fields is far from applicable. Let us for the moment, ignore this defect and take the D_{\max} at face value. We obtain from Fig. 10 the values $\phi_{456} = 89^\circ$ and $\phi_{280} = 85^\circ$, and then from Fig. 9 the values $\chi_{456} = 56^\circ$ and $\chi_{280} = 55^\circ$. This implies that the dipoles are nearly parallel and close to the sagittal plane.

Parallelism, however, is unreasonable in light of a flavin receptor hypothesis. Kurtin and Song (1968) and Siódmiak and Frackowiak (1972) have shown

Figure 10. Theoretical receptor dichroism. D_{\max} , the dichroism or maximum relative differential absorption is plotted as a function of ϕ , the angle between the tangential component of the receptor dipole and the azimuthal axis. D_{\max} was calculated assuming perfectly aligned transition dipoles located on a cylindrical surface for the test angles θ_{\max} and $\theta_{\max} + 90^\circ$.

$$D_{\max} \equiv \frac{A(\theta_{\max}) - A(\theta_{\max} + 90^\circ)}{A(\theta_{\max}) + A(\theta_{\max} + 90^\circ)}$$

where $A(\theta_{\max})$ is the average receptor absorption at \vec{E} orientation = θ_{\max} .

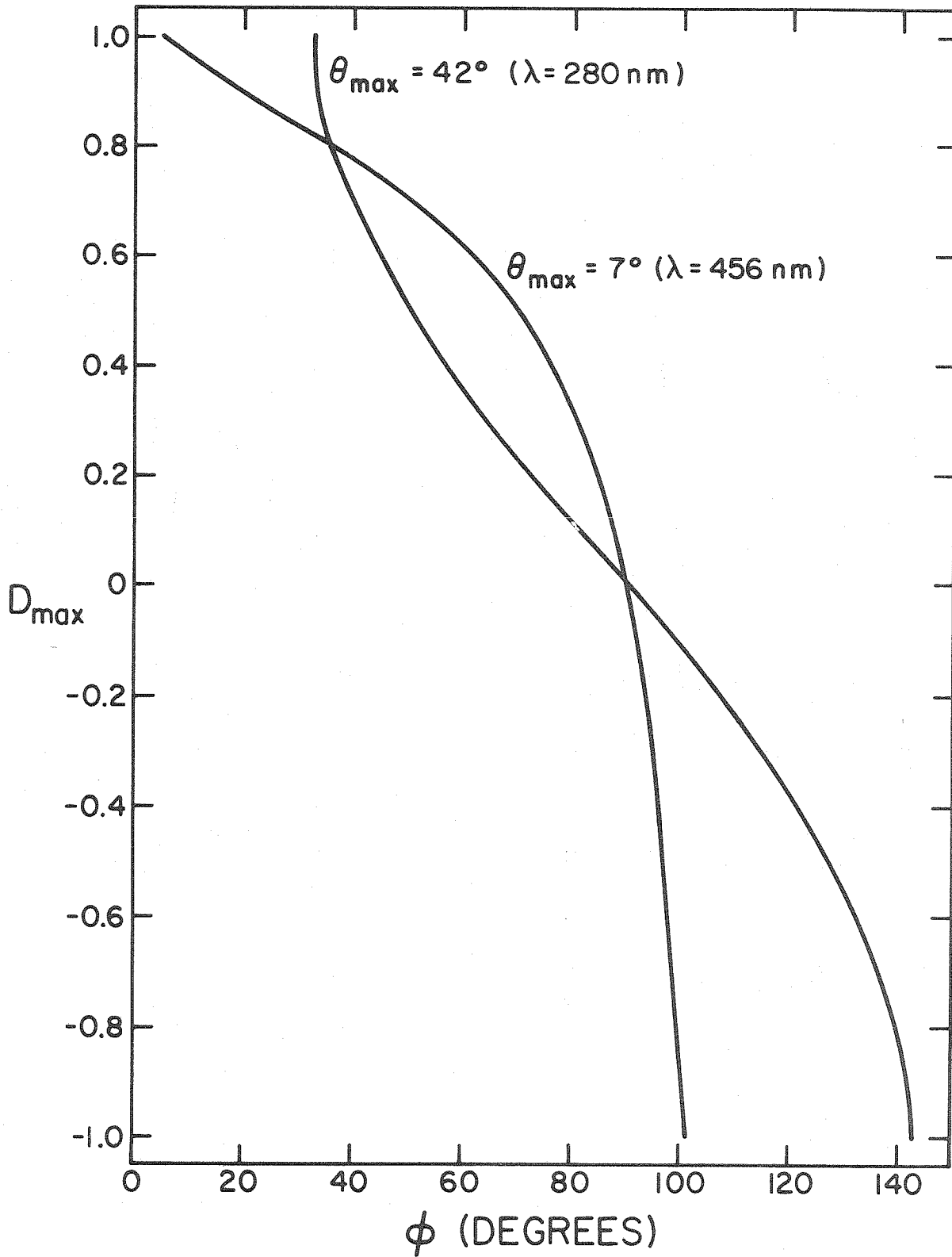
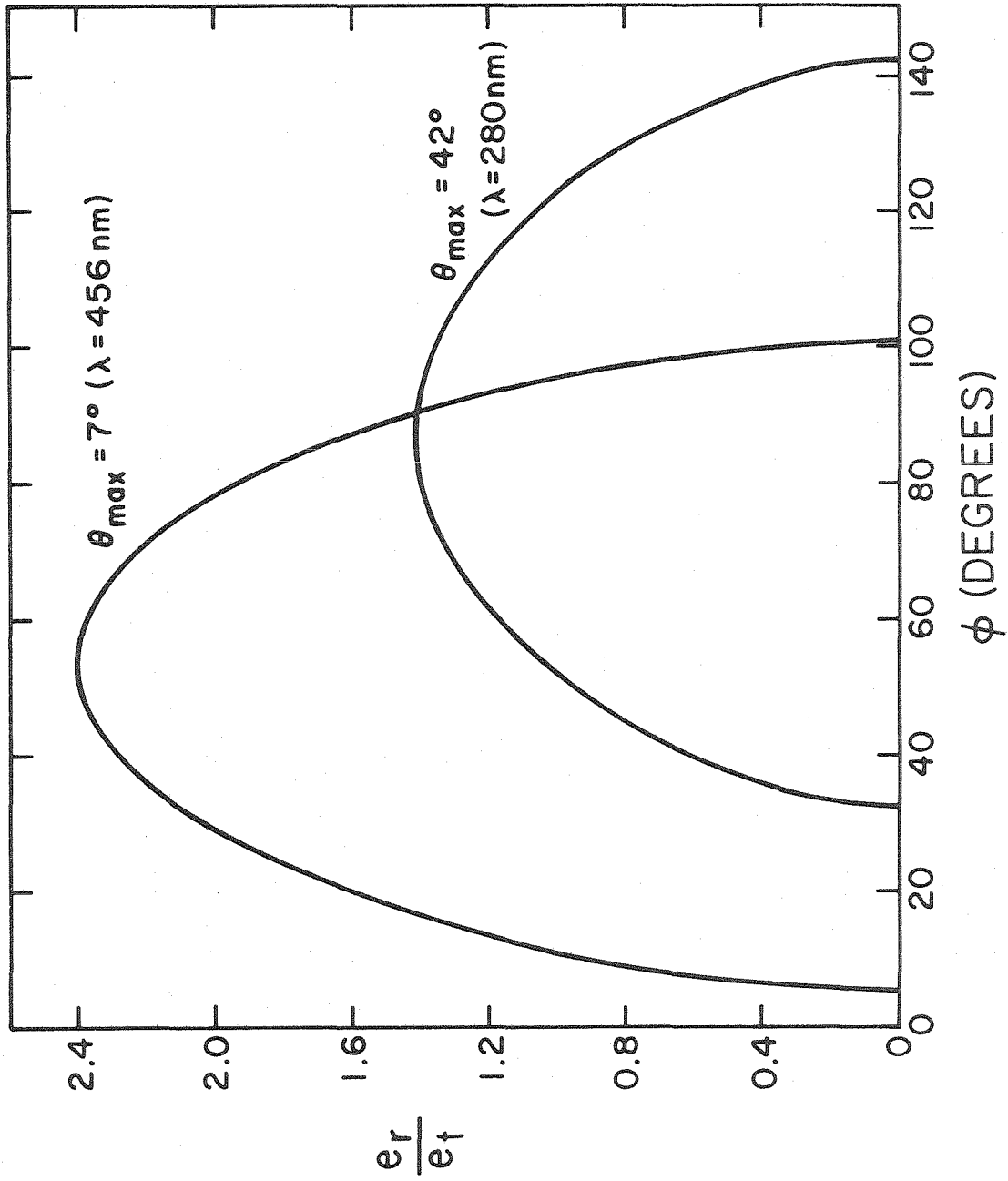


Figure 11. Relative magnitudes of the radial and tangential components of the receptor dipole. e_r/e_t , the quotient of the radial and tangential components is plotted as a function of ϕ for $\theta_{\max} = 7^\circ$ and 42° . e_r/e_t was calculated for the same conditions as stated in Figs. 9 and 10.



that the 270 nm and 450 nm absorption oscillators of riboflavin lie in the plane of the molecule forming an angle of about 60° with each other (Fig. 12). These orientations, moreover, have been shown to be relatively invariant under different molecular geometries (Song et al., 1972). Thus, we discuss next calculations where the assumption of perfectly oriented dipoles has been dropped. Disorientation would reduce the differential absorption, thus explaining the low measured values for D_{\max} .

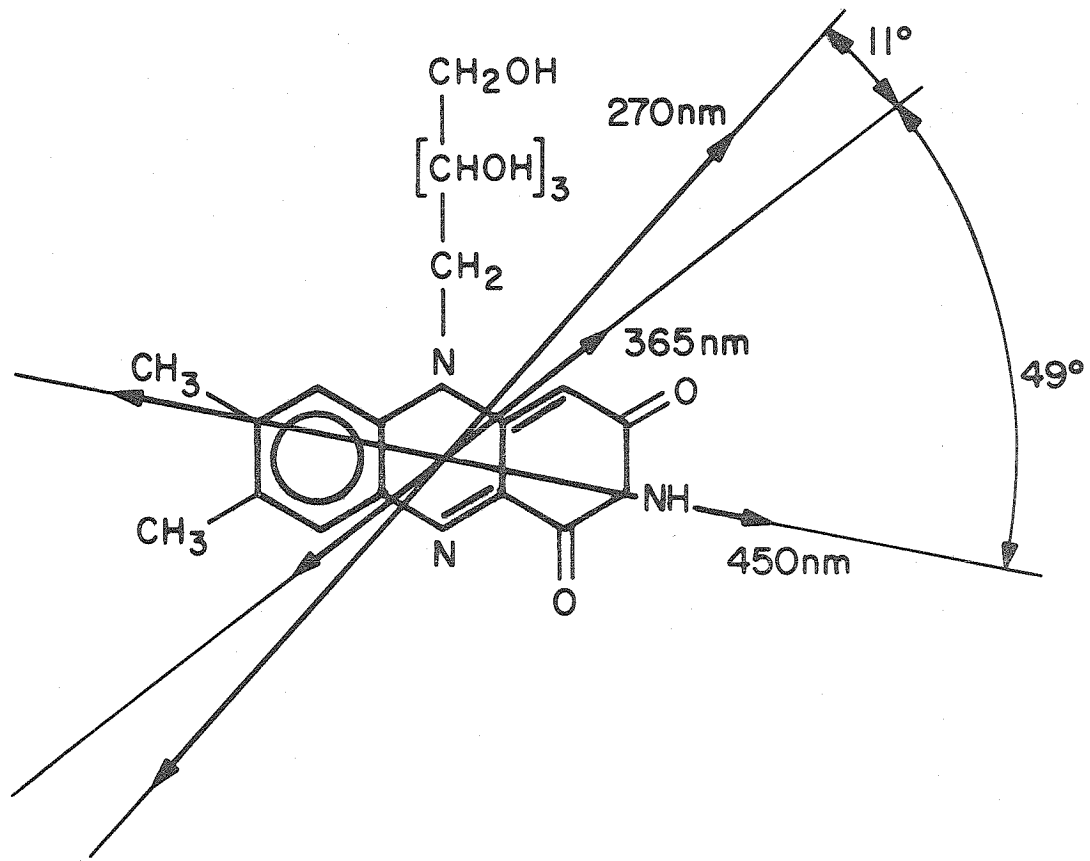
Flavin Receptor, 280 nm and 455 nm dipoles separated by 60°

Because a flavin or flavoprotein is strongly suspected as the photopigment we now wish to analyze a model which constrains the angle between the two dipoles to the known value of flavins.

Assume that:

- (1) a flavin is exclusively responsible for the action spectrum of Phycomyces;
- (2) absorption can be divided into a fraction due to receptors that are perfectly aligned and a fraction due to randomly oriented receptors;
- (3) the random fractional absorption is the same for different transitions of the receptor;
- (4) the angle between and magnitudes of the 280 nm and 456 nm receptor dipoles are the same as for riboflavin. Namely, 60° for the angular separation and 1.3:1 for the ratio of strengths of the 270 nm to the 450 nm transitions (Kurtin and Song, 1968; Siódmiak and Frackowiak,

Figure 12. Assumed directions of transition moments in riboflavin. Based on fluorescence polarization measurements of riboflavin in solution (Kurtin and Song, 1968) and oriented films (Siódmiak and Frackowiak, 1972), and MO calculations on isoalloxazine (Kurtin and Song, 1968). The lengths of the arrows correspond to the intensities of the transitions.



1972) (Fig. 12).

If there exist values of ϕ, χ and e_{280}/e_{456} which satisfy these conditions and those for θ_{\max} , then they will give the orientation of the flavin molecule in the cell and thus imply an agreement with the flavin hypothesis.

The expression relating γ , the angle between the two transition dipoles, to the orientation angles ϕ and χ of each dipole is derived in Appendix IIC:

$$\cos \gamma = \frac{\cos(\phi_{280} - \phi_{456}) + (K_{280} K_{456})^{\frac{1}{2}}}{[(K_{280} + 1)(K_{456} + 1)]^{\frac{1}{2}}} \quad (\text{IIC7})$$

$$\text{where } K = \tan^2 \chi \sin^2 \phi.$$

When combined with equation (IIB6) the requirement $\gamma = 60^\circ$ severely limits the possible pairs of dipole directions. Fig. 13 shows the relationship between ϕ_{280} and ϕ_{456} for $\gamma = 60^\circ$.

Either one or the other ϕ must be close to its respective minimum value to satisfy these conditions. The transition not restricted to the neighborhood of its minimum can take on a broad range of values shown to be permissible for it in Fig. 9.

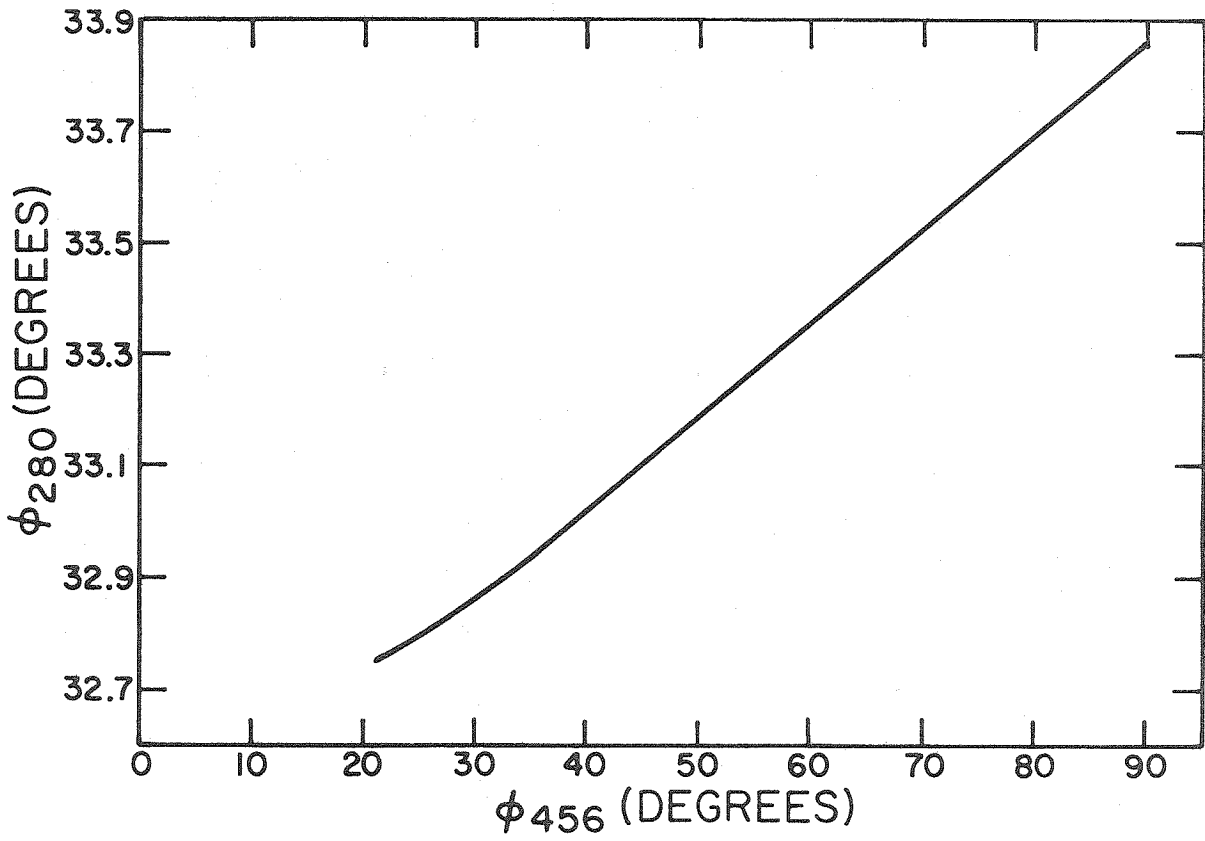
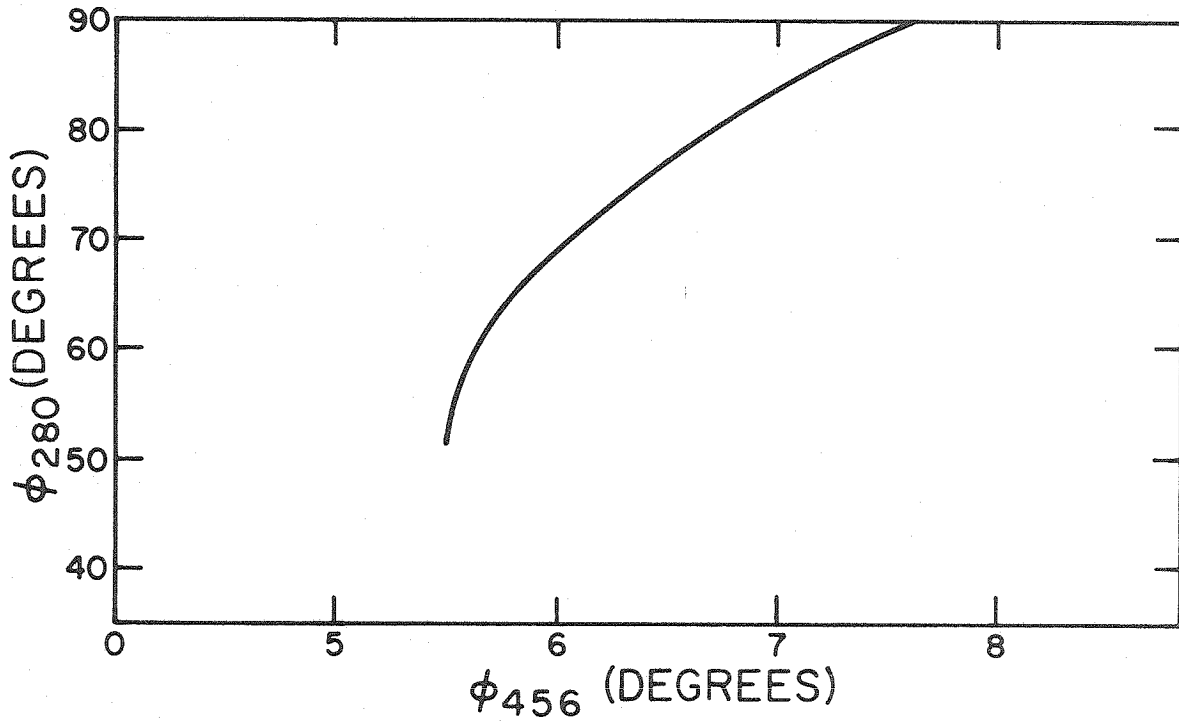
Partially Disordered Receptor Molecules.

If the receptor molecules are permitted to be partially disordered a function $U = U(\phi_{456})$ can be constructed which relates the absorption due to randomly oriented dipoles and their magnitudes (see Appendix IID)

$$U = \frac{A_{456}^{\circ} e_{280}^2}{A_{280}^{\circ} e_{456}^2} \quad (\text{IID9})$$

where A° is absorption due to randomly ordered dipoles

Figure 13. Orientation of tangential components of pairs of receptor dipoles constrained to lie 60° apart. (ϕ_{280}, ϕ_{456}) , defined by these curves, satisfy equations (IIB6) and (IIC7). The corresponding values of χ can be obtained from Fig. 9. Note that the upper curve requires that ϕ_{456} be near its minimum value and that the lower curve requires this for ϕ_{280} .



and $e^2 = \vec{e} \cdot \vec{e}$ or the square of their magnitude.

$U = 1$ expresses the constraint that the ratio: random absorption/square of the dipole's magnitude is the same for the two wavelengths. U is plotted in Fig. 14. For most of the dipole pairs permitted by the other constraints it is far from unity. It approaches 1 for two pairs of dipoles. These will be called Cases I and II.

Case I

$$U = 0.8 \text{ for } \begin{bmatrix} (\phi, \chi)_{456} = (22, 77^\circ) \\ (\phi, \chi)_{280} = (33^\circ, 0^\circ) \end{bmatrix}$$

Case II

$$U = 1.7 \text{ for } \begin{bmatrix} (\phi, \chi)_{456} = (5.5^\circ, 0^\circ) \\ (\phi, \chi)_{280} = (52^\circ, 51^\circ) \end{bmatrix}$$

In Case I, ϕ_{280} is near its minimum value; in Case II this is true for ϕ_{456} . Allowing for experimental error and inaccuracies in the theory, this result makes a good argument for these extreme values, especially those implying radial ordering for \vec{e}_{456} (Case I).

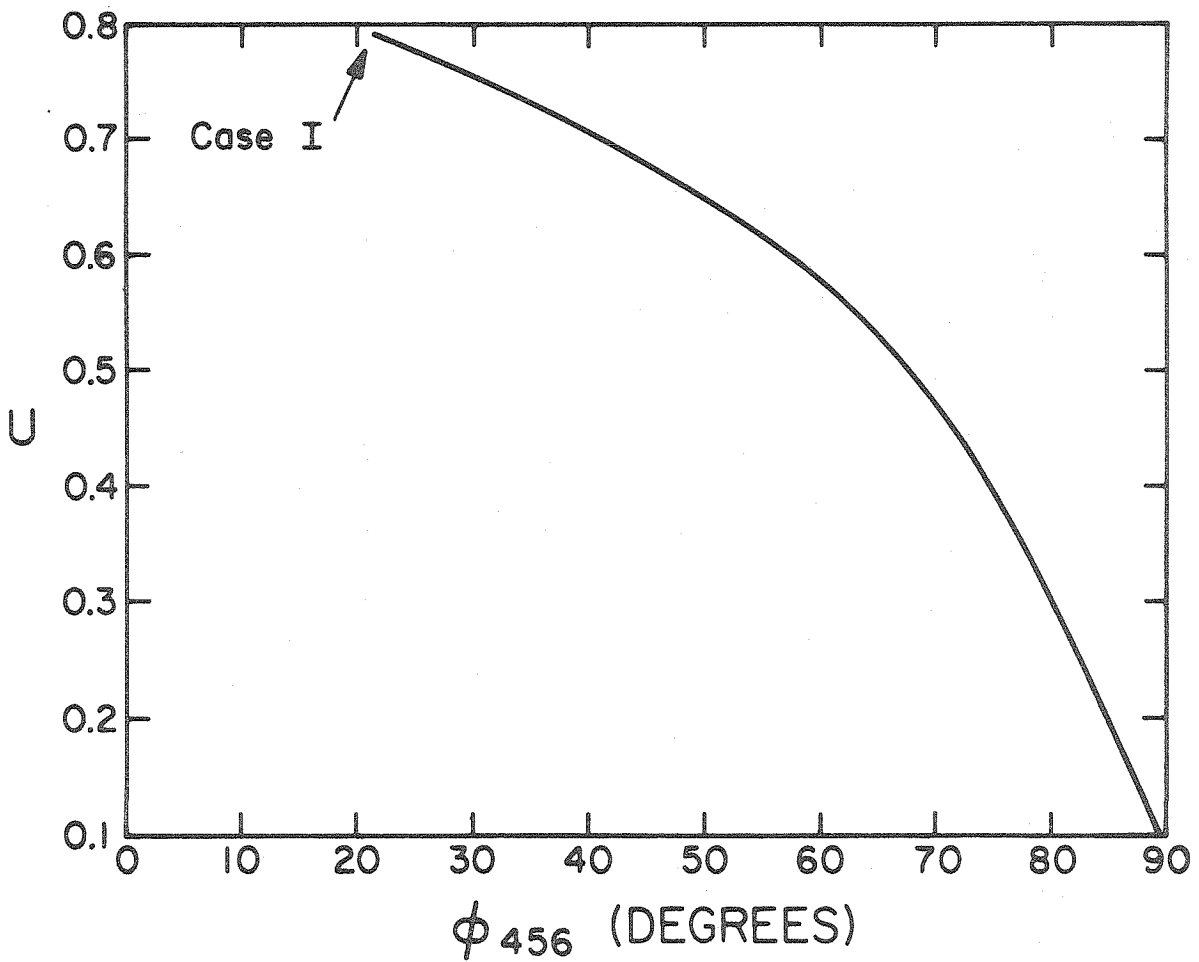
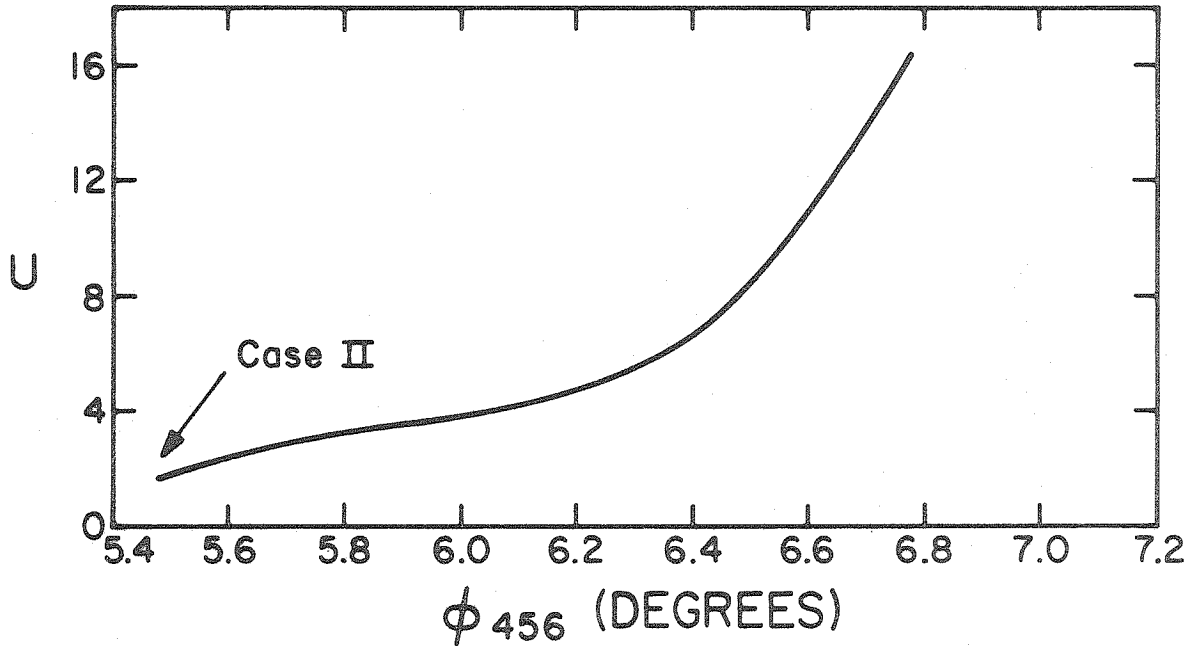
For values of (ϕ, χ) differing appreciably from Case I and II Fig. 14 shows U diverging from 1 quite considerably. This divergence indicates that the above constraints are quite restrictive and that the most probable values are the limiting ones.

We can use the favored values for (ϕ, χ) to calculate the relative absorption due to the oriented and unoriented dipoles. In Appendix IID we see that the quotient of absorption due to oriented dipoles and to disoriented dipoles can be obtained from equation (IID8).

This is simply:

$$\frac{\bar{A}}{A} = \frac{D^t}{D - D^t}$$

Figure 14. Fractional random orientation constraint, U , plotted as a function of ϕ_{456} . For values defined in Fig. 13, U is defined in equation (IID10). If both the 456 nm and 280 nm dipoles have equally disoriented distributions then U should equal 1. Upper curve shows Case II (456 nm dipole is tangential); lower curve shows Case I (280 nm dipole is tangential).



where D^t is the differential absorption for the complete ensemble of dipoles oriented and not. D^t should correspond to the experimental value.

If we let D^t equal to the measured dichroism obtained from the differential response of the sph at $\lambda = 456$ nm and $\lambda = 280$ nm then for

$$\text{Case I} \quad \frac{\bar{A}_{280}}{A_{280}^o} = .06 \quad \text{and} \quad \frac{\bar{A}_{456}}{A_{456}^o} = .07$$

and for

$$\text{Case II} \quad \frac{\bar{A}_{280}}{A_{280}^o} = .1 \quad \text{and} \quad \frac{\bar{A}_{456}}{A_{456}^o} = .06$$

This implies that the absorption due to oriented dipoles accounts for approximately 5 - 10% of the total absorption.

From these calculations it can be said that the measurements of θ_{\max} are compatible with a flavin photoreceptor hypothesis and that either the 456 nm or the 280 nm transition dipoles, but not both, may be oriented wholly tangentially ($\chi = 0$). In either case, the plane of the flavin will be considerably tilted with respect to the tangential plane. If \vec{e}_{456} is tangential then ϕ and χ have the values given above for Case II. If \vec{e}_{280} is tangential then (ϕ, χ) will have the values for Case I. These possibilities are evident in Fig. 14.

In Jaffe's theoretical analysis, it is inferred that aligned tangential ordering for the visible wavelengths is the most likely, since radial ordering cannot explain the fall of the dichroic ratio in a medium of higher refractive index (Shropshire, 1959). Therefore, the tangential ordering of the 456 nm dipole might be favored (Case II).

However, the large experimental error in Shropshire's measured response to polarized light and the fact that the nature of the experiment required that the sph be immersed in a medium totally alien to the sph's normal environment makes this argument a tenuous one.

The assumptions on which these calculations are based are quite reasonable and straight forward, except possibly for the assumption that the photoreceptor pigment in vivo is comprised of a mixture of two populations, a random and a perfectly oriented fraction. It is more likely that it has an average orientation resulting from some kind of constrained molecular rotation and vibration.

The flavin hypothesis is a good one. Flavin absorption matches the *Phycomyces* action spectrum (Bergman et al., 1969), has a high extinction coefficient ($10^4 - 10^5$), and has been shown to participate in complex photochemistry (Penzer et al., 1970). It is now supported by the results for θ_{\max} at 456 nm and 486 nm. The fluorescence polarization spectrum of riboflavin (Kurtin & Song, 1968; Siódmiak and Frackowiak, 1972) possesses a flat region in the 450 nm and 490 nm band. This implies that there is only one major envelope for the transition and the small differences in polarization, and therefore dipole orientation, are due to vibrational levels of the same transition. θ_{\max} for 486 nm and 456 nm are equal, thus agreeing with this observation.

Even if the photoreceptor contained a flavin, however, an additional assumption would be necessary concerning the UV peak of the action spectrum corresponding to flavin absorption. This peak could be due in large part to the protein moiety of the receptor. Calculations

made by Pratt and Butler (1970) indicate that the UV absorbing residues of the protein portion of phytochrome could account for a major part of its extinction coefficient in the ultraviolet. The UV extinction coefficient of riboflavin is approximately equal to that of phytochrome, so if the proteins were at all comparable in their content of UV absorbing residues, then the UV peak of the action spectrum could easily be attributable to the protein. In that case the assumption about the angular separation of the 280 and 456 dipoles would be inappropriate.

More physiological experiments of the type described here should be done to strengthen the flavin hypothesis. If carried out at oblique incidence and repeated for a wavelength of 380 nm (another action spectrum peak), then the true angles between the 3 transition moments could be measured and then compared with the results of Kurtin & Song.

Conclusions

The conclusions may be summarized as follows:

- (1) Phycomyces spphs have greater sensitivity to transversely polarized light because of a dichroic oriented photopigment.
- (2) The pigment molecules must be aligned so that the blue transition moment lies near the equatorial plane of the cell.
- (3) The relative orientations and magnitudes of the spph's response to 280, 456, and 486 nm polarized light is compatible with the idea that the receptor contains a flavin with its molecular plane considerably tilted relative to

the cell wall.

APPENDIX I

Calculation of \bar{r} , σ for the differential growth response

Notation: (refer to Fig. 15)

\bar{V} = average growth rate during an experimental run on an spph

V_i^L = average growth rate during the longitudinal or low intensity interval of the i^{th} cycle

V_i^T = average growth rate during the transverse or high intensity interval of the i^{th} cycle

Z_i^L = total growth during the longitudinal or low intensity interval of the i^{th} cycle

Z_i^T = total growth during the transverse or high intensity interval of the i^{th} cycle

n = number of cycles observed

m = number of spphs observed

σ = standard deviation of the mean

The relative amplitude of growth rate variation for the i^{th} cycle

is r_i^*

$$r_i^* = \frac{(V_i^L - V_i^T)/2}{\bar{V}}$$

Averaging over all cycles we obtain the mean amplitude r , for one

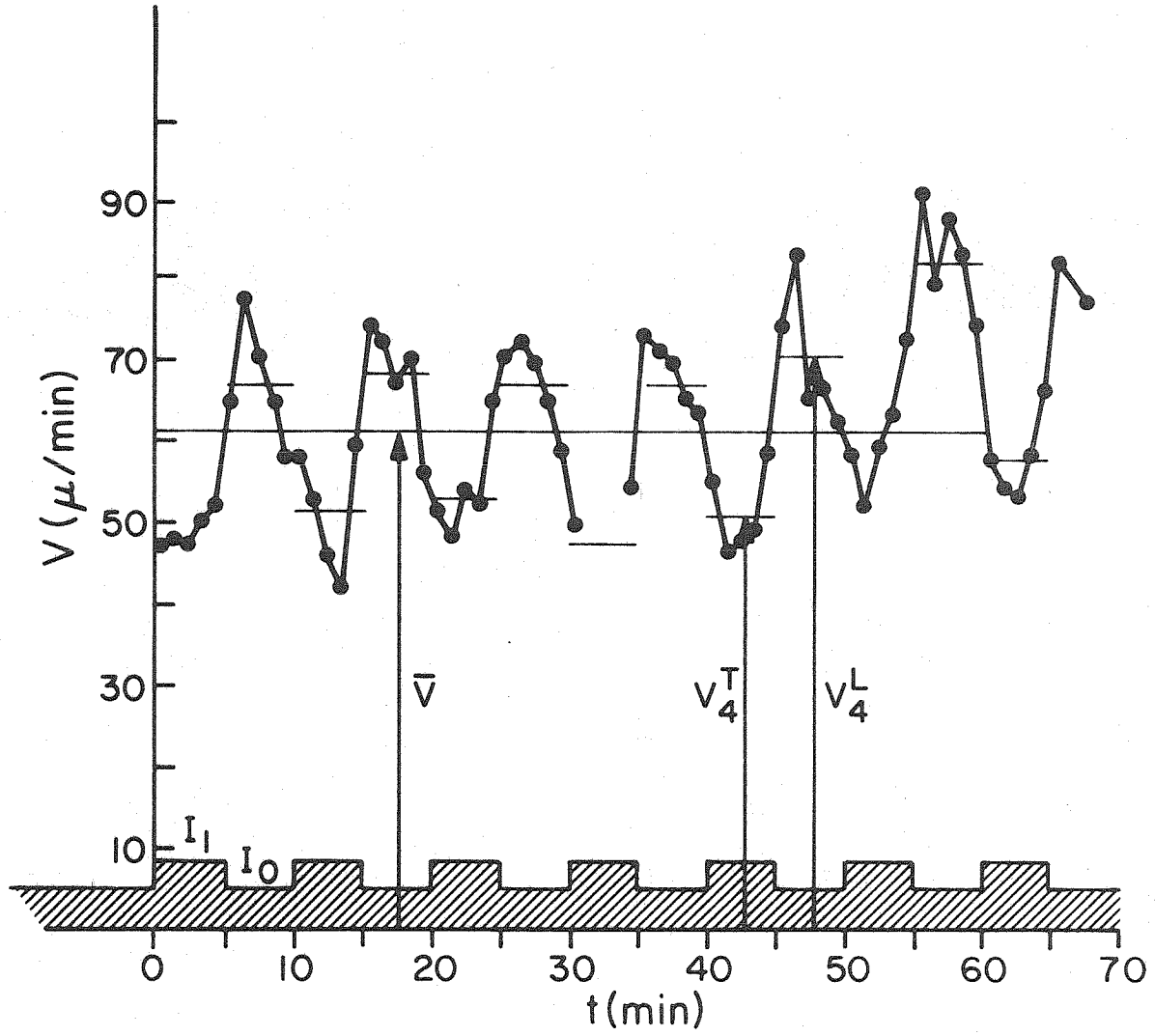
spph

$$r = \frac{\Sigma(V_i^L - V_i^T)/2}{\Sigma(V_i^L + V_i^T)/2} = \frac{\Sigma V_i^L - \Sigma V_i^T}{\Sigma V_i^L + \Sigma V_i^T}$$

But

$$V_i^L = Z_i^L/5 \quad V_i^T = Z_i^T/5$$

Figure 15. Relative amplitude of growth rate variation (r). V , the growth rate of a wild type *spph* is plotted as a function of time. The stimulus program is shown as the hatched area. The height of this region is proportional to the intensity of the stimulus. \bar{V} is the mean growth rate for the first six cycles. V_4^L is the mean growth rate during the low intensity interval of the fourth cycle. V_4^T is the mean growth rate during the high intensity interval of this cycle.



$$r = \frac{\sum Z_i^L - \sum Z_i^T}{\sum Z_i^L + \sum Z_i^T}$$

and

$$\sigma_r = \left(\frac{\sum (r_i^* - r)^2}{n(n-1)} \right)^{\frac{1}{2}}$$

To average these values obtained for each spph, we assume that $r_j = r$ of the j^{th} spph and σ_j is the error of the j^{th} spph belonging to the set

$$\{r_j, \sigma_j \mid j = 1, \dots, m\}$$

Following the procedure for a linear least squares one parameter fit with a priori errors, outlined in Chapter 4 of (Hamilton, 1964), we obtain:

$$\text{mean } \bar{r} = \frac{\sum (r_j / \sigma_j)}{\sum (1 / \sigma_j^2)}$$

$$\text{and } \sigma_{\bar{r}} = \left\{ \frac{1}{m-1} \sum \frac{(r_j - \bar{r})^2}{\sigma_j^2} / \sum \frac{1}{\sigma_j^2} \right\}^{\frac{1}{2}}$$

These values were calculated on the CIT IBM 360/75 computer for all polarization and intensity difference experiments.

APPENDIX IIDipole Orientation and Dichroic Effects.

We introduce two coordinate systems (refer to Figure 16):

(1) x, y, z - the "laboratory" system

y = direction of incident light

x = direction perpendicular to y and to cylinder axis
(transverse)

z = direction parallel to cylinder axis (longitudinal)

(2) r, β, z - the "sph" system

r = radial direction

β = azimuthal direction, perpendicular to cylinder
axis

z = same as in laboratory system

\vec{e} - an absorption transition moment of a receptor molecule
with components e_β, e_r, e_z

e_t - the tangential component of \vec{e} : $e_t^2 = e_\beta^2 + e_z^2$

e - the magnitude of \vec{e}

\vec{E} - the electric vector of polarized light

θ - the angle between \vec{E} and the positive x axis

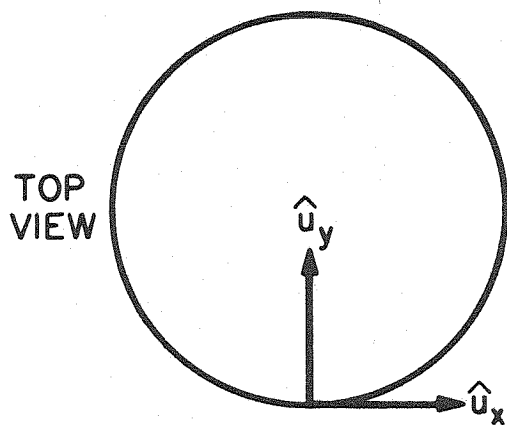
ϕ - the angle between the tangential and azimuthal com-
ponents of \vec{e}

χ - the angle between the sagittal and longitudinal com-
ponents of \vec{e}

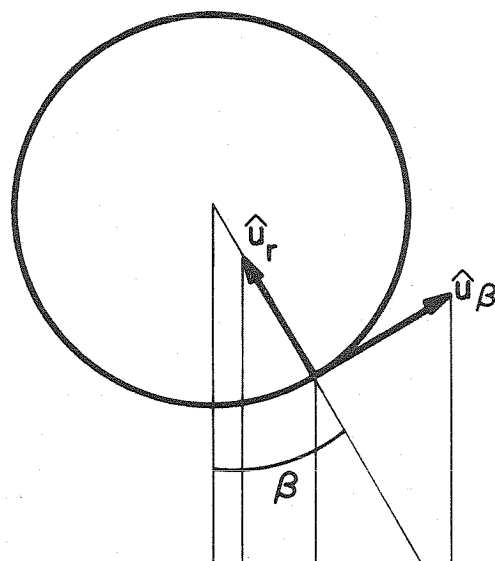
\hat{u}_x , etc - unit vectors in the x -direction, etc.

Figure 16. Coordinate definitions. Schematic top and side views of a sph section are shown. The unit vectors (\hat{u}) of the coordinates used are indicated. Below these, the angles describing the orientation of the \vec{E} and the absorption dipoles are also shown.

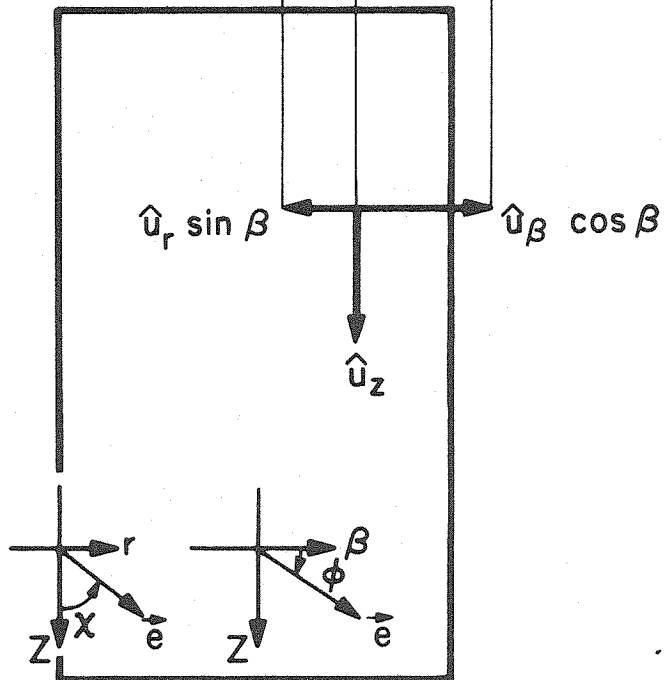
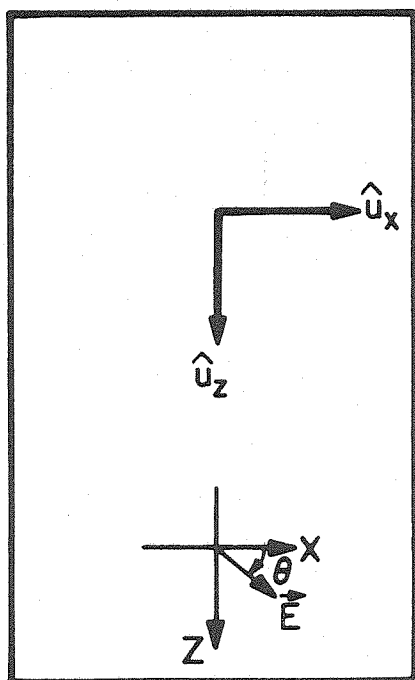
(a)
"LABORATORY"
SYSTEM



(b)
"SPPH" SYSTEM



SIDE VIEW



In the "sph" system the components of the dipole can be written:

$$\vec{e} = \begin{pmatrix} e_\beta \\ e_r \\ e_z \end{pmatrix} = \begin{pmatrix} e_t \cos \phi \\ e_t \sin \phi \tan \chi \\ e_t \sin \phi \end{pmatrix}$$

In the "laboratory" system the components of \vec{E} and the components of a dipole \vec{e} located at the azimuth β can be expressed as follows:

$$\vec{E} = E \cos \theta \hat{u}_x + E \sin \theta \hat{u}_z$$

$$\vec{e} = \begin{pmatrix} \cos \beta & -\sin \beta & 0 \\ \sin \beta & \cos \beta & 0 \\ 0 & 0 & 1 \end{pmatrix} \begin{pmatrix} e_\beta \\ e_r \\ e_z \end{pmatrix} =$$

(The first bracket is the Euler Transformation Matrix for a rotation by the angle β about the z axis.)

$$= (e_\beta \cos \beta - e_r \sin \beta) \hat{u}_x + (e_\beta \sin \beta + e_r \cos \beta) \hat{u}_y + e_z \hat{u}_z$$

The energy absorbed by a dipole is proportional to $(\vec{E} \cdot \vec{e})^2$:

$$\vec{E} \cdot \vec{e} = E \left\{ \cos \theta (e_\beta \cos \beta - e_r \sin \beta) + \sin \theta e_z \right\}$$

$$(\vec{E} \cdot \vec{e})^2 = E^2 \left\{ \cos^2 \theta (e_\beta \cos \beta - e_r \sin \beta)^2 + \sin^2 \theta e_z^2 + \sin 2\theta e_z (e_\beta \cos \beta - e_r \sin \beta) \right\}$$

Let $A(\theta)$ = average absorption of light by a receptor pigment molecule on the proximal side of the sph cylinder (the absorption on the distal side is ignored since the experiments relate to situations in which little light reaches the distal side).

$$A(\theta) = \frac{\int_{-\pi/2}^{\pi/2} (\vec{E} \cdot \vec{e})^2 d\beta}{\int_{-\pi/2}^{\pi/2} d\beta} =$$

$$A(\theta) = \frac{E^2}{2} \left\{ \cos^2 \theta (e_\beta^2 + e_r^2) + \sin^2 \theta (2e_z^2) + \sin 2\theta \left(\frac{4}{\pi} e_z e_\beta \right) \right\} \quad (1)$$

When \vec{E} is at $\theta+90^\circ$

$$A(\theta+90^\circ) = \frac{E^2}{2} \left\{ \sin^2 \theta (e_\beta^2 + e_r^2) + \cos^2 \theta (2e_z^2) - \sin 2\theta \left(\frac{4}{\pi} e_z e_\beta \right) \right\} \quad (2)$$

Now we are in position to calculate for any perfectly aligned dipole field, the

A. Relative differential absorption, (D)

$$\begin{aligned} D(\theta) &= \frac{A(\theta) - A(\theta+90^\circ)}{A(\theta) + A(\theta+90^\circ)} = \quad (3) \\ &= \frac{\cos 2\theta (e_\beta^2 + e_r^2 - 2e_z^2) + \sin 2\theta \left(\frac{8}{\pi} e_z e_\beta \right)}{e_\beta^2 + e_r^2 + 2e_z^2} \end{aligned}$$

in terms of the parameters ϕ, χ this becomes:

$$D(\theta, \phi, \chi) = \frac{\cos 2\theta (\cos^2 \phi - 2\sin^2 \phi + \tan^2 \chi \sin^2 \phi) + \sin 2\theta \left(\frac{4}{\pi} \sin 2\phi \right)}{1 + \sin^2 \phi + \tan^2 \chi \sin^2 \phi} \quad (4)$$

For a given θ , for instance the value of θ at which D is a maximum, this equation expresses a relation between ϕ and χ .

B. The angle of maximum D, (θ_{\max})

For a given dipole field D has a maximum ($=D_{\max}$) for a particular

θ ($=\theta_{\max}$). To calculate θ_{\max} let

$$d = \cos^2 \phi + 2\sin^2 \phi + \tan^2 \chi \sin^2 \phi$$

$$a = \frac{d - 4\sin^2 \phi}{d}$$

$$b = \frac{(4/\pi)\sin 2\phi}{d}$$

With this notation we have

$$D(\theta) = a \cos 2\theta + b \sin 2\theta.$$

Notice that $D(\theta)$ can be considered as the scalar product of two vectors:

$$\vec{V}_1 = (\cos 2\theta, \sin 2\theta)$$

$$\vec{V}_2 = (a, b) \quad (\text{a vector independent of } \theta).$$

The product will have a maximum, as a function of θ , when \vec{V}_1 is parallel to \vec{V}_2 , i.e., when

$$\frac{\sin 2\theta_{\max}}{\cos 2\theta_{\max}} = \frac{b}{a}.$$

Substituting for a and b and dividing numerator and denominator by $\cos^2 \phi$ yields:

$$\tan 2\theta_{\max} = \frac{(8/\pi) \tan \phi}{1 + \tan^2 \phi (\tan^2 \chi - 2)}. \quad (5)$$

For a given θ_{\max} this equation expresses a second relationship between χ and ϕ which can be written in the form

$$\tan^2 \chi = 2 + (8/\pi) \cot \phi \cot 2\theta_{\max} - \cot^2 \phi.$$

χ is plotted as a function of ϕ in Fig. 9 for the values of θ_{\max} experimentally determined at the wavelengths 280 nm, 456 nm, and 486 nm. Using this relation between ϕ and χ , D_{\max} is then plotted in Fig. 10 as a function of ϕ for the same two θ_{\max} .

C. The angle, γ , between absorption dipoles, \vec{e}_1 and \vec{e}_2

Let \vec{e}_1 and \vec{e}_2 be two vectors characterized by the position angles ϕ_1, χ_1 , and ϕ_2, χ_2 .

The angle between two vectors is related to their scalar product:

$$\vec{e}_1 \cdot \vec{e}_2 = e_1 e_2 \cos \gamma$$

$$\begin{aligned} e_1 e_2 \cos \gamma &= e_1^\beta e_2^\beta + e_1^r e_2^r + e_1^z e_2^z \\ &= e_1^t e_2^t (\cos \phi_1 \cos \phi_2 + \sin \phi_1 \sin \phi_2) + e_1^r e_2^r \end{aligned}$$

To express e^t and e^r as functions of e and the position angles, we let

$$K \equiv \left(\frac{e^r}{e^t}\right)^2 = \tan^2 \chi \sin^2 \phi, \text{ and consider that}$$

$$e^2 = e_t^2 + e_r^2 = e_t^2 (1 + K); \quad e_r = e_t \sqrt{K};$$

$$\therefore e_t^2 = \frac{e^2}{K+1}$$

$$\therefore \cos \gamma = \frac{\sqrt{K_1 K_2} + \cos(\phi_1 - \phi_2)}{\sqrt{(K_1 + 1)(K_2 + 1)}} \quad (7)$$

Equation 6, 7 together determine permissible pairs of sets of (ϕ, χ) 's for \vec{e}_1 and \vec{e}_2 . These are shown in Figure 13 for $\gamma = 60^\circ$.

D. Mixture of aligned and randomly oriented dipoles

$A^\circ \equiv$ absorption due to randomly oriented dipoles, independent of θ

$A(\theta) \equiv$ absorption due to the aligned dipoles

$A^t(\theta) \equiv$ total absorption $\equiv A^\circ + A(\theta)$

$D^t(\theta) \equiv$ total relative differential absorption (should correspond to the measured value)

$$A^t(\theta+90) = A(\theta+90) + A^\circ$$

$$D^t(\theta) = \frac{A^t(\theta) - A^t(\theta+90^\circ)}{A^t(\theta) + A^t(\theta+90^\circ)} = \frac{A(\theta) - A(\theta+90^\circ)}{A(\theta) + A(\theta+90^\circ) + 2A^\circ}$$

But $D(\theta) = \frac{A(\theta) - A(\theta+90^\circ)}{A(\theta) + A(\theta+90^\circ)}$ as in equation (4)

Combining the last two equations we obtain, for each transition

dipole a relation between the part of the absorption, A° , due to disordered receptor molecules and the part due to aligned ones:

$$A^\circ = \left(\frac{D}{D^t} - 1 \right) \frac{[A(\theta) + A(\theta+90^\circ)]}{2} = \left(\frac{D}{D^t} - 1 \right) \bar{A}, \quad (8)$$

where \bar{A} is average oriented absorption at θ and $\theta + 90^\circ$.

We assume that the dipoles \vec{e}_1 and \vec{e}_2 belong to the same receptor molecule and are equally disoriented.

$$\therefore \frac{A_1^\circ}{A_2^\circ} = \frac{\vec{e}_1 \cdot \vec{e}_1}{\vec{e}_2 \cdot \vec{e}_2} \quad (9)$$

$$\frac{A_1^\circ}{A_2^\circ} = \left(\frac{e_1}{e_2} \right)^2 = \frac{\left(\frac{D_1}{D_1^t} - 1 \right) [A_1(\theta_1) + A_1(\theta_1+90^\circ)]}{\left(\frac{D_2}{D_2^t} - 1 \right) [A_2(\theta_1) + A_2(\theta_1+90^\circ)]}$$

Substituting equations (1) and (2)

$$\left(\frac{e_1}{e_2} \right)^2 = \frac{\left(\frac{D_1}{D_1^t} - 1 \right) (e_{\beta 1}^2 + e_{r 1}^2 + 2 e_{z 1}^2)}{\left(\frac{D_2}{D_2^t} - 1 \right) (e_{\beta 2}^2 + e_{r 2}^2 + 2 e_{z 2}^2)} =$$

or in terms of D , ϕ , and $K = \tan^2 \chi \sin^2 \phi$

$$\left(\frac{e_1}{e_2} \right)^2 = \frac{\left(\frac{D_1}{D_1^t} - 1 \right) (\cos^2 \phi_1 + 2 \sin^2 \phi_1 + K_1) (K_2 + 1)}{\left(\frac{D_2}{D_2^t} - 1 \right) (\cos^2 \phi_2 + 2 \sin^2 \phi_2 + K_2) (K_1 + 1)} \left(\frac{e_1}{e_2} \right)^2 \quad (10)$$

Thus, the coefficient of $(e_1/e_2)^2$ on the righthand side must be equal to unity if the constraint of equal disorientation of the

two dipoles, e.g. (9), applies. Let us call this coefficient U:

$$(e_1/e_2)^2 = U(\phi_1, \chi_1, \phi_2, \chi_2, D_1^t, D_2^t) (e_1/e_2)^2$$

This function has been calculated for the pairs of dipoles specified in Fig. 13. The values of D_1 and D_2 for these dipoles were taken from eq. (4), and the values of D^t from experiment.

Fig. 14 shows U as a function of ϕ_1 , for the family of dipole pairs permitted under constraints (6) and (7). ϕ_1 corresponds to ϕ_{456} and ϕ_2 to ϕ_{280} .

The values for Fig. 9 - 14 were calculated on the CIT PDP-10 time sharing system.

PART II

FLUORESCENCE STUDIES

PURPOSE

Part II is a summary of an attempt to detect Phycomyces photopigment fluorescence excited at high and low intensities of 488 nm laser light. It is purposely brief since the study, requiring more sensitive and expensive instrumentation, was incomplete. It is intended to serve as an outline for further research at a better equipped laboratory.

INTRODUCTION

From physiological experiments it is known that the Phycomyces spp photoreceptors are dichroic and oriented. Attempts at isolating the photopigment using absorption spectroscopy have been unsuccessful because of its low concentration (10^{-6} - 10^{-7} M) in the cell (Bergman et al., 1969, p.135). The orientation and dichroic nature of the pigment now provides an additional handle with which the pigment may be identified, localized, and perhaps isolated. With this in mind an attempt is being made to physically measure this orientation and dichroism.

Since the pigment is oriented, it seems likely that it is fixed to a membrane surface in the cell. The outer cytoplasmic membrane (the plasmalemma) offers a most probable site. Furthermore, the facility with which this membrane and the accompanying cell wall can be separated from the rest of the cytoplasm makes it ideal for study.

The low concentration of the pigment necessitates the study of its fluorescent properties rather than its absorption properties. Fluorescence techniques offer a tremendous gain in sensitivity because the observation takes place at a different wavelength from the excitation. There are two major disadvantages to this approach, however. First, the fluorescent emission must compete with the biological function of the pigment. Presumably, the organism has evolved a highly efficient light trapping apparatus with a quantum efficiency for the photoresponse of close to one. Consequently, most of the energy absorbed is utilized to trigger the response and only a small part, say one percent, is dissipated. Of that one percent, only a fraction will be emitted as visible fluorescence while the rest is lost as

radiationless transitions, as heat. Therefore, only a very faint fluorescence can be expected and very sensitive equipment must be used.

The second disadvantage is that there may be other substances in the cell which fluoresce, thus masking the pigment fluorescence. The techniques devised should make it possible to discriminate this small component of pigment fluorescence from the rest.

Judging from the action spectrum of Phycomyces, flavoproteins and carotenes are likely candidates for the photopigment. The discovery of fully responsive caroteneless mutants further limits this hypothesis to just flavoproteins. In any cell there are many flavins and flavoproteins which would fluoresce in the same wavelength regions as the photopigment. The majority of these reside in the cytoplasm. Removing the cytoplasm by washing squeezed or burst spps eliminates most of these unwanted flavin components. What remains is the cell wall and plasmalemma in which a sizable fraction of the fluorescent components may be photopigment.

The small size of the spps, the necessity that the cell wall-membrane be separated from the cytoplasm, and the requirement that the region studied be flat and homogeneous demand that a microfluorometric technique, adaptable for polarization measurements, be used.

MATERIALS AND METHODS

Fig. 17 outlines the apparatus used.

Apparatus

A Ziess Ultraphot II microscope was adapted for use as a micro-fluorimeter by using a laser as an external excitation source and by fitting a custom built photomultiplier tube housing to the camera brackets. The specimens were mounted on quartz slides and cover slips and irradiated from above by use of a metallurgical epi-illumination nosepiece.

The exciting light was focussed onto the specimen at near normal incidence, to a spot approximately 75 μm in diameter. The beam divergence was less than 0.05 rad. (3°). The average intensity of the spot was estimated to be approximately 10 watt/cm².

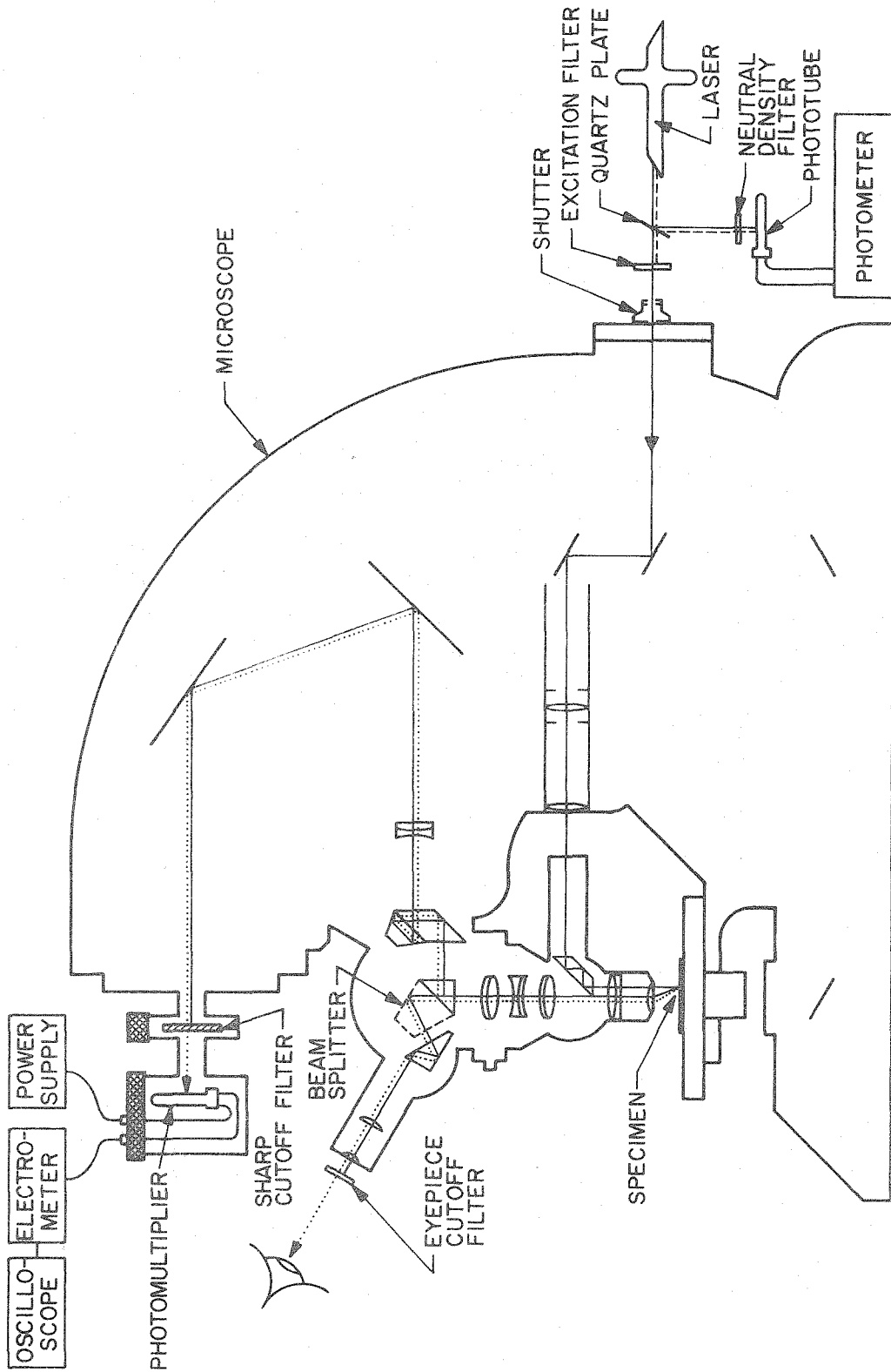
Fluorescence excited by such light could be observed by eye through the eyepiece of the microscope fitted with an eyepiece cutoff filter. To make quantitative measurements a prism could be slipped into the beam to direct the light to the photomultiplier tube filtered with a sharp cutoff filter (520 nm). The tube rested in a light-tight housing fixed to the backing where a ground glass screen normally resides for photography.

Specimens and Preparation

Wild type, C2, C148 (Bergman, et al., 1973) and S18 (Cerdá-Olmedo, 1973) strains were used for these fluorescence studies. Live, squeezed (Castle, 1938), and burst (Oort and Roelofsen, 1932) stage IVb and centrifuged (Zalokar, 1969) stage I spphs were

Figure 17. Microfluorimeter.

- BEAM SPLITTER - To direct light to the eyepiece or P M tube or both.
- ELECTROMETER - Keithley 200B to amplify P M tube current.
- EXCITATION FILTER - Corning 5-61 broad band blue to cut out incoherent red laser cathode light.
- EYEPIECE CUTOFF FILTER - Kodak Orange 0302.
- LASER - RCA argon ion continuous wave laser, tuned to 6 mw power output at 488 nm, vertically polarized.
- MICROSCOPE - Zeiss Ultraphot II used with the epi-illumination nose-piece and H-Pr-Pol reflector insert. Objectives used were Zeiss epiplan pol 16x or 40x.
- NEUTRAL DENSITY FILTER - O.D. = 2.
- OSCILLOSCOPE - Tektronix 502 with camera.
- PHOTOMETER - Eldorado 201 to measure phototube current.
- PHOTOMULTIPLIER - RCA 1P28 run at 900v.
- PHOTOTUBE - RCA 935 to monitor laser intensity.
- POWER SUPPLY - Keithley 240 regulated high voltage supply--for P M tube current.
- QUARTZ PLATE - partially reflecting (7.5%).
- RAYS, DASHED (-----) - Optical path of laser cathode light.
- RAYS, DOTTED (.....) - Optical path of fluorescent light.
- RAYS, SOLID (————) - Optical path of exciting light.
- SHARP CUTOFF FILTER - Schott OG515 in combination with Kodak Orange 0302 acetate sheet--to eliminate exciting light (488nm--cut-off at 520 nm).
- SHUTTER - controlling entrance of laser beam into microscope opening.
Time = 3 msec.
- SPECIMEN - Spph or part mounted in distilled H₂O on fused silica slide and coverslip--Amersil commercial grade T08--to minimize background fluorescence.



mounted on quartz slides and coverslips in distilled water. The squeezed and burst preparations were first washed several times in distilled water. The slide was then placed on the stage and, using physiologically inactive red light, the specimen was brought into focus and centered in the laser beam target area. After shutting off the red light, the light path to the photomultiplier was open by means of the microscope beam splitter. The shutter blocking the laser beam was then opened, allowing the exciting light to reach the specimen.

Fluorescence Measurements

Transient fluorescent changes were recorded by photographing oscilloscope traces during the course of laser excitation. Fifteen second exposures to laser light were repeated after various periods of dark to check for dark regeneration.

Fluorescence polarization was measured only in squeezed and burst spps. After the fluorescence reached a steady state value the specimens were rotated 360° in the polarized excitation beam and the intensity of the fluorescence measured in 10° or 20° increments of rotation.

Fluorescence was also investigated at low intensities of exciting light by expanding the laser beam, using a lower power objective, and several adjacent spps (to fill the field).

RESULTS

Fluorescence from wall preparations (Fig. 18a,b) indicates that there is a fluorescent component in the cell wall or plasma membrane that is 75% bleached in 30 seconds by 488 nm light of intensity 10 watt/cm². It regenerates to 50% of its original value after repeated exposures. It is present in the growing zone and is not present outside the growing zone. This suggests that the fluorescence activity observed is linked to an active process in the cell and is not an artifact.

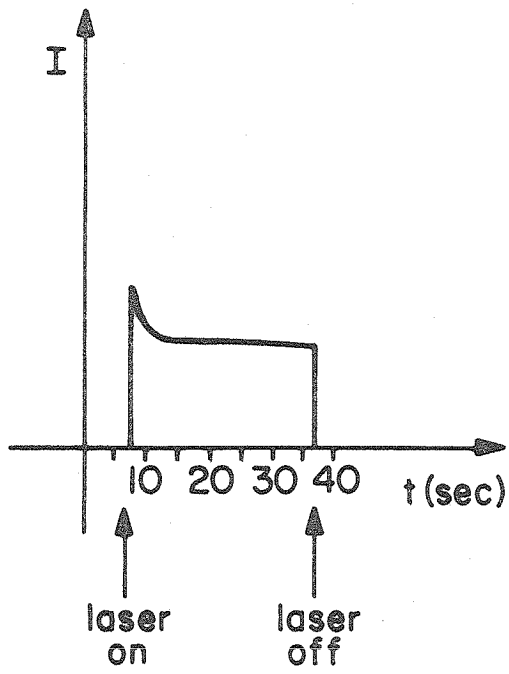
Fluorescence decay also exists in live preparations. It differs from the activity seen in the cell wall fractions in that it is five to ten times more intense, decays to a lesser degree, and regenerates nearly completely. Spph squeezates and aqueous solutions of riboflavin (unstable in 488 nm light show a similar behavior, while rhodamine B in ethylene glycol (stable and highly fluorescent) shows no decay. These facts imply that most of the fluorescence in the live spphs is cytoplasmic in origin and that the regeneration is caused by diffusion of unirradiated material into the spot area.

The tenfold increase in signal in the mitochondrial layer of the centrifuged stage I spph gives some support to the idea that flavins may be the emmitters of this fluorescence. Mitochondria are the metabolic centers of the cell and, therefore, should have a higher concentration of free and bound flavins.

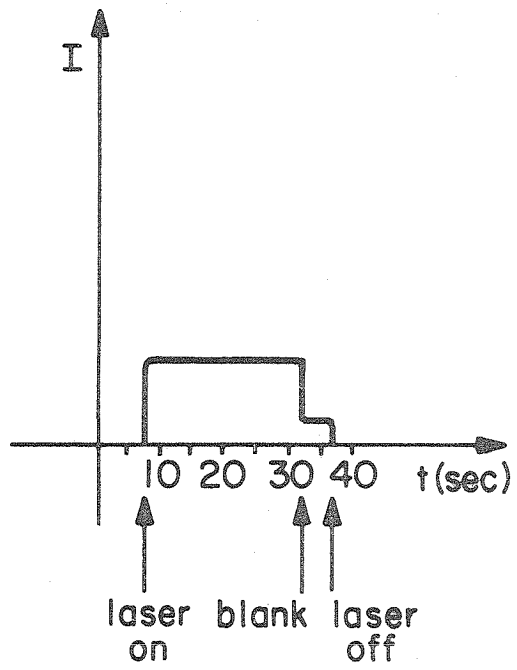
Fluorescence polarization data (Fig. 18c,d) show that there is a fluorescent substance in the cell wall or plasma membrane which is oriented and dichroic. It fluoresces with a different intensity for

Figure 18. Fluorescence decay and polarization results.

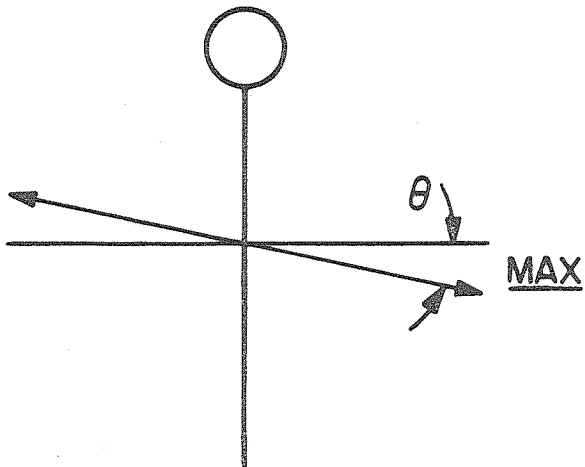
(a) Oscilloscope trace of the rise, and decay of fluorescence from the growing zone of a squeezed C2 sph preparation and (b) outside the growing zone. (c) Angle at which \vec{E} must be oriented in order to give a maximum fluorescent intensity ($12^\circ \pm 15^\circ$ to the transverse axis) and (d) minimum intensity ($109^\circ \pm 12^\circ$).



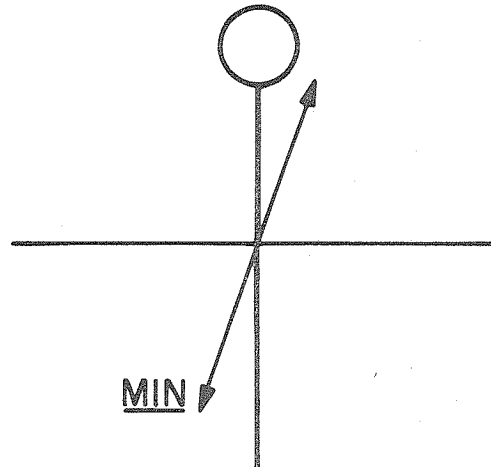
(a)



(b)



(c)



(d)

different orientations of the electric vector of the exciting light relative to the longitudinal axis of the spph. The angle of maximum excitation occurs at 12° to the transverse axis (with a maximum variation through 90° of approximately 28%) in the single layer of cell wall plasmalemma. In the double layer prep (squeezed spph) these values are 0° and 40%. (The direction and magnitude of the maximum excitation agrees with the physiological data.)

In order to eliminate the possibility that this variation is not produced by scattering of light from the transversely oriented chitin microfibrils in the wall, this measurement must be repeated in a medium of matching refractive index (~ 1.50). Calculations show, however, that scattering should produce the opposite effect (Kerker, 1969).

The night blind mutants all show the same fluorescence decay behavior as C2. Polarization was not investigated in these strains.

At laser light intensities less than 100 mw/cm^2 no fluorescence was detectable in live C2 spph. In wild type spph fluorescence became detectable at about 10 mw/cm^2 . No decay was observed.

DISCUSSION AND CONCLUSION

Distribution of the fluorescence decay across the length of the spph and the magnitude and angular variation of polarized excitation of fluorescence imply that the emitter may be the photopigment or its photoproduct. The major objection to these measurements and conclusions is that the intensity of the exciting light is much too high. At an intensity of 10 watts/cm² (quantum flux 2.5×10^{19} quanta/sec at 488 nm) the number of excitations/molecule-sec, assuming a capture cross-section of 1.5×10^{-16} cm², typical for photopigments, is 3.8×10^3 . This means that the photopigment must necessarily be completely bleached in the order of milliseconds. Thus, it is highly unlikely that the fluorescence is derived from excitation to the lowest excited singlet state. This would only be possible if the estimate for the extinction coefficient is too high. Since it is believed that photosensitive organisms would evolve only highly efficient light trapping systems (e.g. rhodopsin), this latter possibility seems unlikely.

The other possibility is that the pigment is completely bleached and that the fluorescence is derived from the excitation of the bleached state. If this state is colorless, the very small absorption coefficient could explain the low quantum yield of fluorescence that has been estimated (3×10^{-5}). This is reasonable since at these intensities substances normally not considered fluorescent are highly fluorescent.

If the first hypothesis is true, then by lowering the intensity by a factor of 10^4 the number of excitations/molecule-sec would be one.

Expecting a quantum efficiency of 0.98 for bleaching and $10^{-3} - 10^{-4}$ for fluorescence, the number of photons emitted per molecule and per growing zone of the cell wall-plasmalemma, can be estimated. These are $10^{-3} - 10^{-4}$ /sec-molecule and $10^5 - 10^6$ /growing zone. The latter quantity is near the sensitivity limit of the instrument.

Experiments at low intensities of exciting light indicate that fluorescence is too weak to be detectable on this instrument. There are systems much superior in sensitivity and capabilities to the crude one described here. It is hoped that this work can be repeated on a more sensitive instrument and extended with excitation and emission spectra.

BIBLIOGRAPHY

- Batra, P. P. 1971. Mechanism of light induced carotenoid synthetis in plants. *Photophysiol.* 6: 47-76.
- Bergman, K., A. P. Eslava, and E. Cerda-Olmedo. In press. Mutants of *Phycomyces* with abnormal phototropism. *Mol. Gen. Gent.*
- Bergman, K., Patricia V. Burke, E. Cerda-Olmedo, C. N. David, M. Delbrück, K. W. Foster, E. W. Goodell, M. Heisenberg, G. Meissner, M. Zalokar, D. S. Dennison, and W. Shropshire, Jr. 1969. *Phycomyces*. *Bacteriol. Rev.* 33: 99-157.
- Blasie, J. K., and C. R. Worthington. 1969. Planar liquid like arrangement of photopigment molecules in frog retinal receptor disk membranes. (1969). *J. Mol. Biol.* 39: 417-439.
- Blasie, J. K. 1972. The location of photopigment molecules in the cross-section of frog retinal receptor disk membranes. *Biophys. J.* 12: 191-204.
- Castle, E. S. 1934. The phototropic effect of polarized light. *J. Gen. Physiol.* 17: 41-47.
- Castle, E. S. 1938. Orientation of structure in the cell wall of *Phycomyces*. *Protoplasma* 31: 331-345.
- Cerdá-Olmedo, E. In press. *Phycomyces*. In: R. C. King (ed.), *Handbook of Genetics*. Van Nostrand Reinhold, New York.
- Clayton, R. K. 1965. Phototaxis in microorganisms. *Photophysiol.* 2: 51-77.
- Delbrück, M., and W. Shropshire, Jr. 1960. Action and transmission spectra of *Phycomyces*. *Plant Physiol.* 35: 194-204.
- Hamilton, W. C. 1964. *Statistics in Physical Science*. Ronald Press Co., New York.

- Haupt, W., G. Mörtel, and I. Winkelkemper. 1969. Demonstration of different dichroic orientations of phytochrome P_r and P_{fr} . *Planta* 88: 183-186.
- Hsu, Wan-Jean. 1973. Personal communication.
- Jaffe, L. F. 1958. Tropistic responses of zygotes of the Fucaceae to polarized light. *Exp. Cell Res.* 15: 282-299.
- Jaffe, L. F. 1960. The effect of polarized light on the growth of a transparent cell. A theoretical analysis. *J. Gen. Physiol.* 43: 897-911.
- Jaffe, L. F., and H. Etzold. 1962. Orientation and locus of tropic photoreceptor molecules in spores of *Botrytis* and *Osmunda*. *J. Cell Biol.* 13: 13-31.
- Jaffe, L. F., and H. Etzold. 1965. Tropic responses of *Funaria* spores to red light. *Biophys. J.* 5: 715-742.
- Kerker, M. 1969. *The Scattering of Light, and other electromagnetic radiation.* p.255-310. Academic Press, New York.
- Kurtin, W. E., and P.-S. Song. 1968. Photochemistry of the model system involving flavins and indoles.--I. Fluorescence polarization and MO calculations of the directions of the electronic transition moments in flavins. *Photochem. Photobiol.* 7: 263-273.
- Lees, A. D. 1968. Photoperiodism in insects. *Photophysiol.* 4: 47-137.
- Liebman, P. 1962. In situ microspectrophotometric studies on the pigments of single retinal rods. *Biophys. J.* 2: 161-178.
- Meissner, G., and M. Delbrück. 1968. Carotenes and retinal in *Phycomyces* mutants. *Plant Physiol.* 43: 1279-1283.

- Menke, W. 1963. Experiments made to elucidate the molecular structure of chloroplasts, p. 537-544. In: NAS-NRC Publication 1145. Symposium on Photosynthetic Mechanism of Green Plants.
- Nebel, B. J. 1969. Responses of moss protonema to red and far red polarized light. Evidence for disc shaped phytochrome photoreceptors. *Planta (Berl.)* 87: 170-179.
- Olson, R. A. 1963. Oriented molecules and the structure of chloroplasts. p. 545-559. In: NAS-NRC Publication 1145. Symposium on Photosynthetic Mechanisms of Green Plants.
- Oort, A. J. P., and P. A. Roelofsen. 1932. Spiralwachstum, Wandbau, und Plasmastromung bei *Phycomyces*. *Koninkl. Ned. Akad. Wetenschap. Proc.* 35: 898-908.
- Ootaki, T., Anita Crafts-Lighty, M. Delbrück, and Wan-Jean Hsu. 1973. Complementation between mutants of *Phycomyces* deficient with respect to carotenogenesis. *Molec. Gen. Genet.* 121: 57-70.
- Penzer, G. R., G. K. Radda, J. A. Taylor, and M. B. Taylor. 1970. Chemical properties of flavins in relation to flavoprotein catalysis. In: R. S. Harris, P. L. Munson, and E. Diczfalusy (ed.), *Vitamins and Hormones.* 28: 441-446.
- Pickett, J. M., and C. S. French. 1967. The action spectrum for blue light-stimulated oxygen uptake in *Chlorella*. *Proc. Natl. Acad. Sci. U.S.* 57: 1587-1593.
- Pratt, L. H., and W. L. Butler. 1970. Phytochrome conversion by ultraviolet light. *Photochem. Photobiol.* 11: 503-509.
- Robinson, G. W. 1966. Excitation transfer and trapping in photo-

- synthesis. p. 16-48. In: Brookhaven Symposia in Biology: No. 19. Energy Conversion by the Photosynthetic Apparatus.
- Roelofsen, P. A. 1951. Cell wall structure in the growth-zone of *Phycomyces sporangiophores*. II. Double refraction and electron microscopy. *Biochim. Biophys. Acta.* 6: 357-373.
- Seliger, H. H., and McElroy, W. D. 1965. Light: Physical and Biological Action. p. 56-79. Academic Press, New York.
- Shropshire, W., Jr. 1959. Growth Responses of *Phycomyces* to polarized light stimuli. *Science* 130: 336.
- Siódmiak, J., and D. Frackowiak. 1972. Polarization of fluorescence of riboflavin in anisotropic medium. *Photochem. Photobiol.* 16: 173-182.
- Song, P.-S., T. A. Moore, and W. E. Kurtin. 1972. Molecular luminescence studies of flavins, II. Interactions involving excited states. *Z. Naturforsch.* 27b: 1011-1015.
- Thomas, J. B. 1965. Primary Photoprocesses in Biology. p. 225-243. John Wiley & Sons, Inc., New York.
- Voskrenskaya, N. P. 1972. Blue light and carbon metabolism. *Ann. Rev. Plant Physiol.* 23: 219-234.
- Waterman, T. H. 1966. Polarotaxis and primary photoreceptor events in Crustacea, p. 493-511. In: G. G. Bernhard (ed.). *The Functional Organization of the Compound Eye*. Pergamon Press, Oxford.
- Waterman, T. H., H. R. Fernandez, and T. H. Goldsmith. 1969. Dichroism of photosensitive pigment in rhabdoms of the crayfish *Orconectes*. *J. Gen. Physiol.* 54: 415-432.

- Zalokar, M. 1969. Intracellular centrifugal separation of organelles in *Phycomyces*. *J. Cell. Biol.* 41: 494-509.
- Zankel, K. L., P. V. Burke, and M. Delbrück. 1967. Absorption and screening in *Phycomyces*. *J. Gen. Physiol.* 50: 1893-1906.
- Zimmerman, W. F. and D. Ives. 1971. Some photophysiological aspects of circadian rhythmicity in *Drosophila*. p. 381-391. In: *Biochronometry*, ISBN 0-309-01866-8. National Academy of Sciences. Washington, D.C.
- Zurzycki, J. 1967a. Properties and localization of the photoreceptor active in displacements of chloroplasts in *Funaria hygrometrica*. II. Studies with polarized light. *Acta Soc. Bot. Pol.* 36: 143-151.
- Zurzycki, J. 1967b. Properties and localization of the photoreceptor active in displacements of chloroplasts in *Funaria hygrometrica*. III. Cytochemical studies. *Acta Soc. Bot. Pol.* 36: 617-625.